David Oliveira Borges

Licenciado em Ciências da Engenharia
Electrotécnica e de Computadores

Low complexity detection for SC-FDE massive MIMO systems

Dissertação para obtenção do Grau de Mestre em
Engenharia Electrotécnica e de Computadores

Orientador: Prof. Dr. Rui Dinis, Professor Associado com Agregação,
Faculdade de Ciências e Tecnologia - UNL

Co-orientador: Prof. Dr. Paulo Montezuma, Professor Auxiliar,
Faculdade de Ciências e Tecnologia - UNL

Júri:

Presidente: Prof. Dr. Luís Oliveira – FCT/UNL

Vogais: Prof. Dr. Luís Bernardo – FCT/UNL (Arguente)

Prof. Dr. Paulo Montezuma – FCT/UNL

FACULDADE DE
CIÊNCIAS E TECNOLOGIA
UNIVERSIDADE NOVA DE LISBOA

Setembro, 2016

Low complexity detection for SC-FDE massive MIMO systems

O saber não ocupa lugar.

Agradecimentos

Aos professores e orientadores desta tese Rui Dinis e Paulo Montezuma por toda a paciência e disponibilidade que demonstraram no decorrer desta tese. Por todo o conhecimento, motivação e boa disposição, obrigado.

À minha família, agradeço pela confiança e motivação para nunca desistir, por tudo o que fizeram por mim a nível pessoal e académico, estiveram sempre ao meu lado para me dar força nos bons e maus momentos.

A todos os amigos que, mais de perto ou não tanto, estiveram presentes no decorrer deste percurso académico, que tantos bons momentos nos proporcionou, beijinhos e abraços.

Agradeço também o apoio da Fundação da Ciência e Tecnologia, através da bolsa de investigação BI_110_15 no âmbito do projeto PHY-MAC.

Abstract

Nowadays we continue to observe a big and fast growth of wireless communication usage due to the increasing number of access points, and fields of application of this technology. Furthermore, these new usages can require higher speed and better quality of service in order to create market. As example we can have: live 4K video transmission, M2M (Machine to Machine communication), IoT (Internet of Things), Tactile Internet, between many others.

As a consequence of all these factors, the spectrum is getting overloaded with communications, increasing the interference and affecting the system's performance. Therefore a different path of ideas has been followed and the communication process has been taken to the next level in 5G by the usage of big arrays of antennas and multi-stream communication (MIMO systems) which in a greater scale are called massive MIMO schemes. These systems can be combined with an SC-FDE (Single-Carrier Frequency Domain Equalization) scheme to improve the power efficiency due to the low envelope fluctuations.

This thesis focused on the equalization in massive MIMO systems, more specifically in the FDE (Frequency Domain Equalization), studying the performance of different approaches, namely ZF (Zero Forcing), EGD (Equal Gain Detector), MRD (Maximum Ratio Detector), IB-DFE (Iterative Block Decision Feedback Equalizer) and a proposed receiver combining MRD (or EGD) and IB-DFE.

With this approach we want to minimize the ICI (Inter Carrier Interference) in order to have almost independent data streams and to produce a low complexity code, so that the receiver's performance doesn't affect the total system's performance, with a final objective of increasing the data throughput in a great scale.

Keywords: 5G, massive MIMO, Single-Carrier, Frequency-Domain Equalization

Resumo

Hoje em dia continuamos a assistir a um grande e rápido crescimento da utilização da comunicação sem fios, devido ao aumento do número de pontos de acesso e campos de aplicação desta tecnologia. Além do aumento na transferência de dados, os novos tipos de utilização podem exigir uma maior velocidade e melhor qualidade de serviço, seja por necessidade dos utilizadores ou por necessidade de mercado. Como exemplo, podemos ter: transmissão em direto de vídeo 4K, M2M (comunicação máquina a máquina), IoT (Internet das coisas), Internet Táctil, entre muitas outras.

Como consequência do aumento do número de utilizadores, o espectro está a ficar sobrecarregado com comunicações, aumentando a interferência. Desta forma, um caminho diferente de ideias tem sido seguido e o processo de comunicação foi levado para um próximo nível no 5G, com o uso de grandes conjuntos de antenas e vários fluxos de dados (sistemas MIMO), que em maior escala são chamados de MIMO massivo.

Estes sistemas podem ser combinados com a técnica SC-FDE (Mono portadora com igualização na frequência) para o *up-link* de modo a melhorar a eficiência energética devido às baixas flutuações na envolvente do sinal. Esta tese incidirá sobre o campo de igualização, mais especificamente em FDE (Igualização no domínio da frequência), estudando o desempenho de diferentes abordagens, nomeadamente ZF (Zero Forcing), EGD (Equal Gain Detector), MRD (Maximum

Ratio Detector), IB-DFE (Iterative Block Decision Feedback Equalizer) e uma proposta de recetor combinando MRD (ou EGD) e IB-DFE. Com esta abordagem queremos minimizar a interferência, de modo a obtermos fluxos de dados quase independentes, e produzir um código de baixa complexidade para que o desempenho do recetor não afete o desempenho total do sistema, com um objetivo final de aumentar a taxa de transferência de dados.

Palavras-chave: 5G, MIMO massivo, Mono-portadora, Igualização no Domínio da Frequência.

ACRONYMS

3G 3rd Generation

3GPP 3rd Generation Partnership Project

4G 4th Generation

5G 5th Generation

BER Bit Error Rate

BS Base Station

CSI Channel State Information

DFE Decision feedback equalization

DFT Discrete Fourier Transform

DPC Dirty Paper Coding

EGD Equal Gain Detector

FD Frequency Domain

FDE Frequency Domain Equalization

FDM Frequency Division Multiplexing

FFT Fast Fourier Transform

HSPA High Speed Packet Access

IB-DFE Iterative Block Decision Feedback Equalization

IC Interference Cancelation

ICI Inter-Carrier Interference

IFDE Iterative Frequency Domain Equalization

IFFT Inverse Fast Fourier Transform

ISI Inter symbol Interference

LOS Line of sight

LTE Long Term Evolution

MIMO Multiple Input Multiple Output

MMSE Minimum Mean Square Error

MRD Maximum Ratio Detector

MRT Maximum Ratio Transmission

MU-MIMO Multiple User-Multiple Input Multiple Output

OFDM Orthogonal Frequency-Division Multiplexing

OFDMA Orthogonal Frequency-Division Multiple Access

PAPR Peak Average Power Ratio

QoE Quality of Experience

QoS Quality of Service

QPSK Quadrature Phase Shift Keying

RSSI Received signal strength indication

SC Single Carrier

SC-FDE Single-Carrier Frequency Domain Equalization

SNR Signal-to-Noise Ratio

SU-MIMO Single User-Multiple Input Multiple Output

TD Time Domain

TDMA Time Division Multiple Access

UE User Equipment

UMTS Universal Mobile Telecommunication System

Contents

AGRADECIMENTOS ______ **VII**

ABSTRACT ______ **IX**

RESUMO ______ **XI**

ACRONYMS ______ **XIII**

LIST OF FIGURES ______ **XVII**

1 INTRODUCTION ______ **1**

1.1 MOTIVATION AND SCOPE ______ 1

1.2 OBJECTIVES ______ 3

1.3 ORGANIZATION ______ 4

1.4 CONTRIBUTIONS ______ 4

2 MIMO TECHNIQUES FOR SC MODULATION ______ **5**

2.1 GENERAL 5G ______ 5

2.2 AN EXTENSION TO HIGHER FREQUENCY/MILLIMETER WAVES ______ 5

2.3 MIMO ______ 8

2.4 MASSIVE MIMO ______ 10

2.5 SC-FDE ______ 13

2.6 PRECODING ______ 16

2.6.1 Precoding technique ______ 16

2.6.2 Precoding for Multi-user MIMO Systems ______ 17

2.7 SCENARIO CHARACTERIZATION ______ 18

2.7.1 Channel models ______ 21

CONVENTIONAL DETECTION SCHEMES ______ **23**

3.1 OVERALL DISCRETE-TIME MODEL ______ 24

3.2 BASIC COMBINING ALGORITHMS ______ 25

3.2.1 Switching ______ 25

3.2.2 Selection ______ 26

3.2.3 Zero Forcing ______ 27

3.2.4 Equal Gain Combining ______ 29

3.2.5 Maximum Ratio Combining ______ 30

3.3 MINIMUM MEAN SQUARED ERROR ______ 31

3.4 ITERATIVE BLOCK DECISION FEEDBACK EQUALIZER (IB-DFE) ______ 32

3.4.1 IB-DFE with Soft Decisions ____ 35
3.5 SINGULAR VALUE DECOMPOSITION (SVD) ____ 37
4 ITERATIVE MASSIVE MIMO RECEIVERS ____ 39
4.1 EGD/MRD + IB-DFE ____ 40
4.2 PERFORMANCE RESULTS ____ 42
4.2.1 Iterations effect ____ 42
4.2.1.1 Results of iterations effect on EGD ____ 43
4.2.1.2 Results of iterations effect on MRD ____ 44
4.2.1.3 Results of iterations effect on IB-DFE ____ 45
4.2.2 Increasing number of antennas ____ 46
4.2.2.1 Increasing ratio ____ 46
4.2.2.2 Constant ratio ____ 47
4.2.2.3 Increasing transmitting antennas ____ 49
5 CONCLUSIONS ____ 51
5.1 FINAL CONSIDERATIONS ____ 51
5.2 FUTURE WORK ____ 52
ATTACHMENTS ____ 53
BIBLIOGRAPHY ____ 59

List of figures

FIG. 1.1– MULTIPATH PROPAGATION AND TIME DISPERSION EFFECT [4] 2
FIG. 2.1– 4G VS 5G ANTENNA (ACTIVE PHASED-ARRAY ANTENNA). 6
FIG. 2.2 – PHOTO OF THE ANTENNA ARRAY OF THE LUMAMI TESTBED AT LUND UNIVERSITY IN SWEDEN 7
FIG. 2.3 - POSSIBLE LANDSCAPE AND PERFORMANCE AIMS [12]. 8
FIG. 2.4 – MIMO 2X2 CHANNEL CONFIGURATION. 10
FIG. 2.5 - MASSIVE MIMO SCENARIO. 11
FIG. 2.6 - ANTENNA CONFIGURATIONS AND DEPLOYMENT SCENARIOS FOR A MASSIVE MIMO BASE STATION 12
FIG. 2.7 – SC-FDE RECEIVER STRUCTURE [17] ADAPTED.1 14
FIG. 2.8- OFDM VS SC-FDE [20] ADAPTED. 15
FIG 2.9 – TYPICAL TRANSMISSION VS BEAMFORMING WAVES. 18
FIG. 2.10– MASSIVE MIMO UP-LINK SCENARIO. 19
FIG. 3.1– DIVERSITY COMBINING RECEIVER 25
FIG. 3.2 – EXAMPLE OF SWITCHING ALGORITHM SIGNAL ENVELOPE. 26
FIG. 3.3 – EXAMPLE OF SWITCHING ALGORITHM RECEIVER ARCHITECTURE. 26
FIG. 3.4 – EXAMPLE OF SELECTION ALGORITHM SIGNAL ENVELOPE. 26
FIG. 3.5 – EXAMPLE OF SELECTION ALGORITHM RECEIVER ARCHITECTURE. 27
FIG. 4.1– PROPOSED RECEIVER STRUCTURE. 41
FIG 4.2 – ITERATIONS EFFECT ON 20X10 EGD 43
FIG 4.3– ITERATIONS EFFECT ON 50X10 EGD 43
FIG 4.4 – ITERATIONS EFFECT ON 100X10 EGD 43
FIG 4.5– ITERATIONS EFFECT ON 20X10 MRD 44
FIG 4.6– ITERATIONS EFFECT ON 50X10 MRD 44
FIG 4.7– ITERATIONS EFFECT ON 100X10 MRD 44
FIG 4.8– ITERATIONS EFFECT ON 20X10 IB-DFE 45
FIG 4.9– ITERATIONS EFFECT ON 50X10 IB-DFE 45
FIG 4.10 – ITERATIONS EFFECT ON 100X10 IB-DFE 45
FIG 4.11 – INCREASING RATIO EFFECT ON EGC 46
FIG 4.12 – INCREASING RATIO EFFECT ON MRC 46
FIG 4.13– INCREASING RATIO EFFECT ON IB-DFE 47
FIG 4.14 – CONSTANT RATIO EFFECT ON EGC 48
FIG 4.15 – CONSTANT RATIO EFFECT ON MRC 48
FIG 4.16 – CONSTANT RATIO EFFECT ON IB-DFE 48
FIG 4.17 – INCREASING TRANSMITTING ANTENNAS ON EGC 49
FIG 4.18 – INCREASING TRANSMITTING ANTENNAS ON MRC 49
FIG 4.19 – INCREASING TRANSMITTING ANTENNAS ON IB-DFE 49

1

Introduction

1.1 Motivation and Scope

Wireless communications have experienced exponential growth in the last few decades due to the development of reliable solid-state radio frequency hardware in the 1970s. Since then, innumerous standards have been developed for wireless systems throughout the world [1].

The increasing need for fast and reliable wireless communication links has led to some new path of ideas and systems with multiple antennas located at both the transmitter and the receiver side is one of them. Multiple-Input Multiple-Output (MIMO) systems are able to increase very significantly the capacity and hence achieve higher transmission rates than the one-sided array links.

The notorious Shannon theorem for capacity of bandlimited Gaussian channels shows that there is a fundamental limit (channel capacity) for transmission data rate over these channels [2]. With the advances in communication theory and the growth of sophisticated signal processing and computation techniques, the possibility of achieving the fundamental information limit on the channel capacity seems higher than ever before.

The next generation of wireless systems is expected to provide end-to-end communication where voice, data and streamed multimedia can be served to users at "anytime, anywhere" basis with an aim of Gbits/s. Data throughput has long been one of the most important performance indicators for communication systems.

Block transmission techniques have been used intensively due to their performance in high data rate transmission over severely time-dispersive channel. The two mainly used alternatives are OFDM (Orthogonal Frequency Division Multiplexing) and SC (Single Carrier) modulation combined with FDE (Frequency Domain Equalization). This thesis will focus on the SC-FDE technique which is more suitable for uplink due to its lower PAPR (Peak to Average Power Ratio) [3].

As a direct consequence of the increase in data rates, the effects of multipath propagation, inter-symbol interference (ISI) have been augmented, resulting in the need for more complex equalizers. The complexity of the equalization process is enlarged even more in MIMO systems due to the addition of extra transmit and receive antennas.

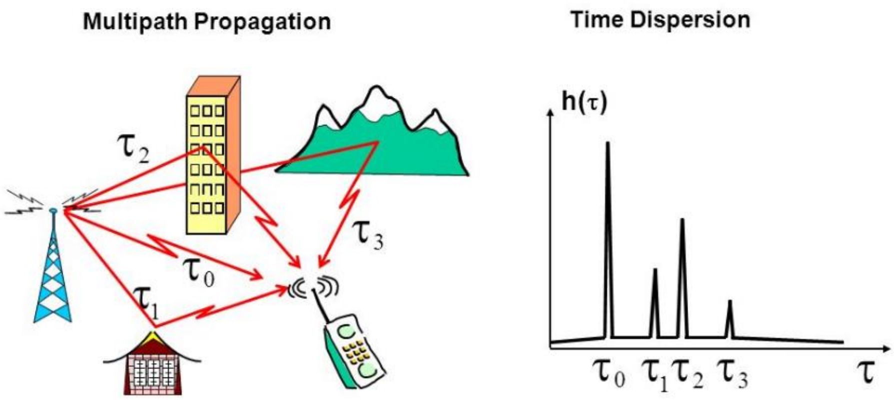

Fig. 1.1– Multipath propagation and time dispersion effect [4].

Before 1990s, multipath effect has been considered for much time one of the main obstacles that prevents high throughput transmission. This effect can be explained in time or frequency domain, and its depicted in Fig. 1.1. In the time domain, the signal arrives to the receiver with different delays, due to the different paths of propagation which can have different obstacles and interferences. The delay measured from the first arriving signal to the last one its called delay spread. This measure is used to calculate the guard interval needed between transmitted symbols to prevent inter-symbol interference (ISI). The insertion of this time interval will limit the transmission data throughput [5]. This multipath effect in the time domain leads to frequency selective fading, hence, if the signal occupied a considerable bandwidth, it will experience the frequency selective fading and the performance of the system will degrade significantly. To overcome the multipath effect and achieve high data rate transmission, channel equalization and precoding can be used. The original principle of precoding is that if the transmitter side knows the channel state information, it can prepare the signal to be transmitted so that the ISI in the receiver side is greatly mitigated. As an example, Tomlinson-Harashima precoding is based on the migration of the feedback part of the DFE (Decision Feedback Equalization) to the transmitter side to avoid the error propagation problem.

All this increased complexity in the analog and digital domain has its disadvantages. This thesis will focus on the receiver design, having in mind the high computational processing needed for massive MIMO schemes. The delay that can be introduced by these complex scenarios is going against the 5G ideology which aims an ultra-low latency. For this reason the complexity of the receivers used in massive MIMO schemes should be as low as possible without compromising the desired QoS.

1.2 Objectives

The objective of this thesis is, based on state of the art technology, to develop and test a low complexity detector for SC-FDE massive MIMO systems. This objective includes the development, test and usage of a massive MIMO system simulator, implementing the scenario described in the next section, in which both proposed receivers were tested. All these tasks were accomplished using a numerical computing environment, MATLAB®.

A low-complexity iterative frequency-domain receiver combined with the MRD (Maximum Ratio Detector) and other based on EGD (Equal Gain Detector) are proposed. These receivers do not require matrix inversions and have excellent performance, being able to approach the MFB (Matched Filter Bound) after just a few iterations, even for a moderate number of antennas.

The receivers were tested and studied by analyzing the impact of the number of used antennas in each sender and receiver at a time. By varying the number of antennas in transmitter and receiver separately, changing the ratio between receiving and transmitting antennas (*R:T*) and ultimately increasing the number at both ends at the same time, different scenario types were analyzed and compared. The BER (Bit Error Rate) values, as well as the performance of different FDE's approaches in BER values were the key features that were observed to take conclusions.

1.3 Organization

This thesis is divided in five sections as described bellow:

Chapter 2 contains an introduction and a literature review about related work and used technologies. An overview about 5G is presented, followed by a description of millimeter wave systems that includes MIMO and massive MIMO. It continues with the explanation of SC-FDE, precoding and its particular usage, beamforming. Chapter ends with the proposed scenario characterization.

In Chapter 3 overall discrete model is presented, basic detections schemes are explained and the receiver's algorithms are introduced.

Chapter 4 contains an overview on iterative massive MIMO receivers and the description of the receivers' proposed model and algorithms. After this, performance results and conclusions are presented.

Finally, Chapter 5 contains the overall conclusions and possible future work that can be done by taking this dissertation as reference.

A paper with the performance analysis of these receivers was produced in the elaboration of this thesis and its presented as an attachment.

1.4 Contributions

During the development of this thesis, after implementing and testing the proposed receivers in simulations, some observed results were considered motivating. In order to validate this interest with the community, a scientific paper a scientific paper was produced and summited to a conference. As this interest was shared among the evaluators, the paper was accepted in the *2016 IEEE Global Conference on Signal and Information Processing* which had place from 7th to 9th of December of 2016 in Greater Washington D.C., USA. It was kindly presented by Prof. Dr. Rui Dinis on the 9th of December.

2

MIMO techniques for SC modulation

2.1 General 5G

Massive MIMO schemes (Multiple-Input, Multiple-Output) involving several tens or even hundreds of antenna elements are expected to be central technologies for 5G systems. The integration of millimeter-wave (mmWave) and MIMO can achieve orders of magnitude increase in rates due to larger bandwidth and greater spectral efficiency [6]. This makes mmWave MIMO as a promising technique for future 5G wireless communication systems. Extremely higher data rates, large BW (Bandwidth) and ultra-low latencies required by 5G wireless cannot be achieved by the simple evolution of current wireless technologies [7].

This chapter characterizes some of the disrupting technologies that will be useful in enabling the 5G transition. Starting by a review of the state of the art, mm-wave systems, MIMO and massive MIMO are explained. Their advantages and obstacles are presented, as well as suitable techniques like SC-FDE and Precoding. It finished with the description of the proposed and simulated general scenario, regarding a massive MIMO communication system.

2.2 An Extension to Higher Frequency/Millimeter Waves

All the frequency spectrums currently available to mobile systems are concentrated in bands below 6 GHz due to the favorable propagation conditions in those bands. These frequencies are also in high demand by other wireless services, including fixed, broadcasting and satellite communications. As a result, these bands have become extremely crowded and prospects for large chunks of new spectrum for mobile telecommunications below 6 GHz are not very favorable for transition to 5G architectures.

4G vs 5G antenna technology

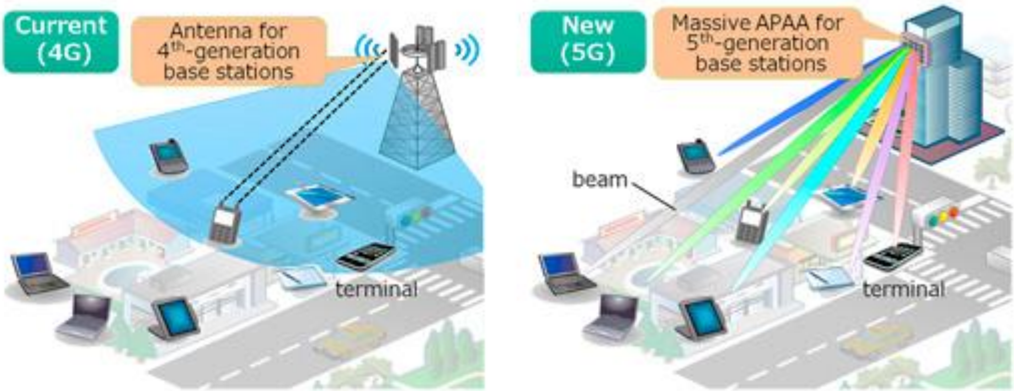

Fig. 2.1– 4G vs 5G antenna (Active Phased-Array Antenna).

Recent advances in mobile communication systems and devices operating at higher microwave and mm-wave frequencies, combined with improvements in antenna and RF component technologies, have opened the doors to using non-conventional bands for cellular applications. Such advancements will help enable dense small cell deployments over a diverse set of higher spectrum bandwidth. Such deployments will be an important 5G's usage scenario as there will be continued need to meet exponential growth in traffic demand and to address the requirement for gigabit data rates everywhere, including at cell edge, as exemplified in Fig. 2.1. It is expected that to meet 5G network requirements, operating over this higher part of spectrum (e.g. 10-100+ GHz) will be needed to deploy indoors and/or outdoors.

With the potential use of frequencies higher than 10 GHz as well as mm-wave deployment, the available spectrum might rise from a typical 500MHz to several GHz, making many bands therein seem promising. Nevertheless, with the increase in carrier frequency, signal penetration loss increases, diffracted signals become very weak and thus the importance of line-of-sight (LOS) signal as well as reflected signal component increases. Although propagation at mm-wave bands covering 30-300GHz presents some challenges, recent measurements indicated distance dependent LOS communication channel characteristics similar to microwave bands. Non-LOS communication remains a good option [8].

Extreme sensitivity to blockages, higher atmospheric attenuation and need for accurate frequency-dependent channels models have created the need for further research to enable mm-wave dense networks and relay infrastructures. Large antenna arrays can be used to eliminate frequency dependent propagation loss and to provide higher beamforming array gain [9].

Millimeter wave systems can operate in noise-limited conditions rather than interference-limited situations by reducing the impact of interference with narrow beam adaptive arrays. When beams are blocked by obstacles, the use of adaptive array processing algorithms can help to adapt quickly. The smaller wavelength associated with higher frequencies of mmWave enables to pack a large antenna array in a small physical dimension, as we can observe in Fig. 2.2 [9]. The large antenna array can provide sufficient antenna gain to compensate for the severe attenuation of mmWave signals due to path loss, oxygen absorption, and rainfall effect [10]. Additionally, the large antenna array can also support the transmission of multiple data streams to improve the spectral efficiency through the use of precoding [11].

Antenna array at Lund University in Sweden

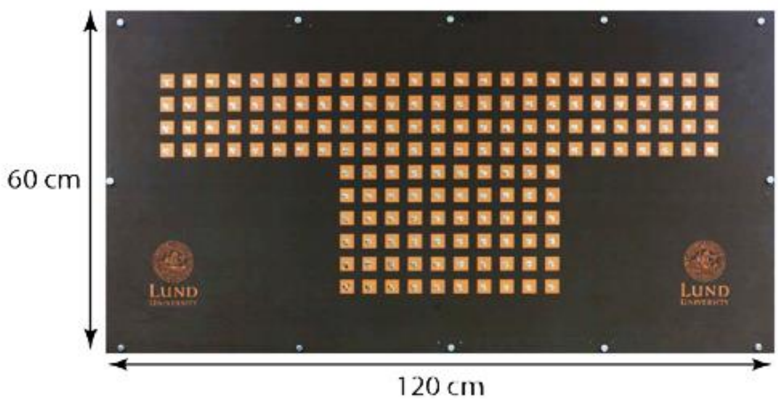

Fig. 2.2 – Photo of the antenna array of the LuMaMi testbed at Lund University in Sweden. The array consists of 160 dual-polarized patch antennas. It is designed for a carrier frequency of 3.7 GHz and the element-spacing is 4 cm (half a wavelength).

Next generation of wireless radio standard, 5G, must deliver radical improvement over current 4G in speed and other functionalities so that it continues to satisfy ever-increasing user expectations of Quality of Experience (QoE). With the predicted 100-1000 fold increase in network capacity, 5G promises to do much more than 4G in terms of denser network coverage, faster download time, HD-video streaming and so on. Fig. 2.3 shows one landscape possibility with some performance requirements envisioned for 5G. The development of Internet of Things (IoT) with tens of billions of connected devices and entities will also fuel the need for better Quality of Service (QoS) that cannot be met just by the LTE evolution. 5G wireless networks are expected to fill the gap with a revolutionary enhancement in user experience [12].

Emerging wide area wireless services and usage cases are shaping the 5G vision and driving the 5G technology requirements. Ultra-high throughput, enhancement in network capacity, ultra-low latency, ubiquitous connectivity, energy efficiency, high reliability, low-cost devices and QoE are just some of the requirements that the next generation wireless needs to achieve. The race is currently on to find the wireless communication network, system architectures, and technologies that will bring the big data to the world beyond 2020.

5G possible landscape and aimed performance

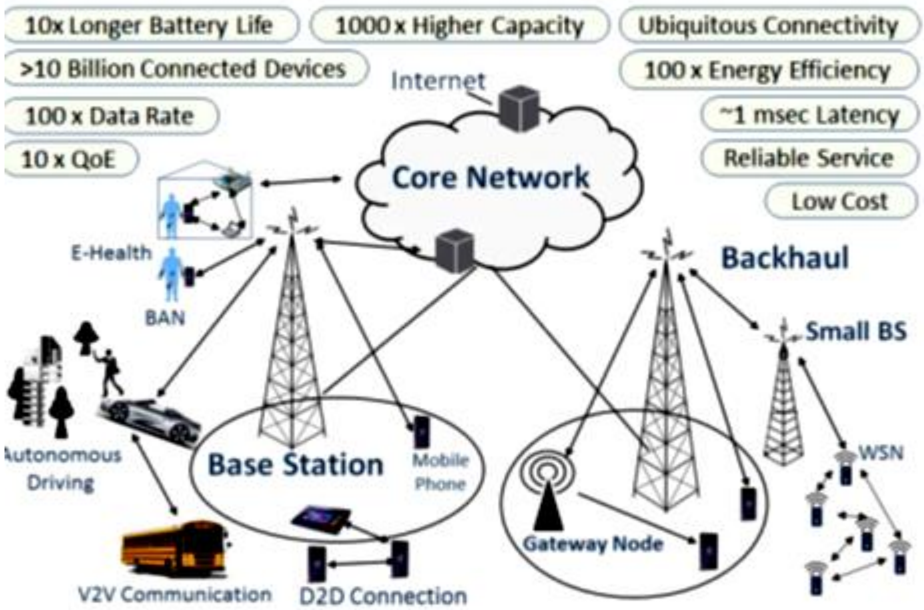

Fig. 2.3 - Possible landscape and performance aims [12].

2.3 MIMO

In communications, MIMO is a technology for increasing the capacity and reliability of a radio link using multiple transmit and receive antennas to exploit multipath propagation. MIMO is often traced back to 1970s research papers concerning multi-channel digital transmission systems and interference (cross-talk) between wire pairs in a cable bundle. The earliest ideas in this field go back to work by A.R. Kaye and D.A. George (1970) and W. van van Etten (1975, 1976). Jack Winters at Bell Laboratories and Jack Salz at Bell Labs published several papers on beamforming related applications in the mid-eighties 1984, 1986. Arogyaswami Paulraj and Thomas Kailath proposed the concept of Spatial Multiplexing using MIMO in 1993. In 1996, Greg Raleigh and Gerard J. Foschini refine new approaches to MIMO technology. Nowadays it has become an essential element of wireless communication standards including IEEE 802.11n (Wi-Fi), IEEE

802.11ac (Wi-Fi), HSPA+ (3G), WiMAX (4G), and Long Term Evolution (4G LTE). More recently, MIMO has been applied to power-line communication for 3-wire installations as part of ITU G.hn standard and HomePlug AV2 specification.

At one time in wireless the term "MIMO" referred the mainly theoretical use of multiple antennas at both the transmitter and the receiver. In modern usage, "MIMO" specifically refers to a practical technique to send and receive several data signals on the same radio channel, at the same time, via multipath propagation. In Fig. 2.4 we can observe what it would be a channel configuration of 2 transmitting and 2 receiving antennas in a MIMO scheme. MIMO is fundamentally different from smart antenna techniques developed to enhance the performance of a single data signal, such as beamforming and diversity [13]. MIMO applied in cellular systems brings four improvements:

- **increased data rate**: due to the usage of more antennas, the more independent data streams can be transmitted and the more terminals can be served simultaneously;
- **enhanced reliability**: increasing number of transmitting antennas creates more distinct paths for the radio signal to propagate over;
- **improved energy efficiency**: the base station can focus its emitted energy into the spatial directions where it knows that the terminals are located;
- **reduced interference**: the base station can purposely avoid transmitting into directions where spreading interference would be harmful.

Other benefits of massive MIMO include the extensive use of inexpensive low-power components, reduced latency, simplification of the media access control (MAC) layer, and robustness to intentional jamming. All improvements cannot be achieved simultaneously, and there are requirements on the propagation conditions, but the mentioned bullets are the general benefits.

MIMO technology for wireless communications in its conventional form is maturing, and incorporated into recent and evolving wireless broadband standards. The more antennas the base station (or terminals) are equipped with, and the more degrees of freedom that the propagation channel can provide, the better performance in all the above four aspects—at least for operation in time-division duplexing (TDD) mode. However, the number of antennas used today is modest. The most modern standard, LTE-Advanced, allows for up to 8 antenna ports at the base station and the mobile terminals being built today have much fewer antennas than that [14]. The gains in multiuser systems (MU-MIMO) are even more impressive, because such systems offer the possibility to transmit simultaneously to several users and the flexibility to select what users are scheduled to be received at any given point in time.

General 2x2 MIMO channel configuration

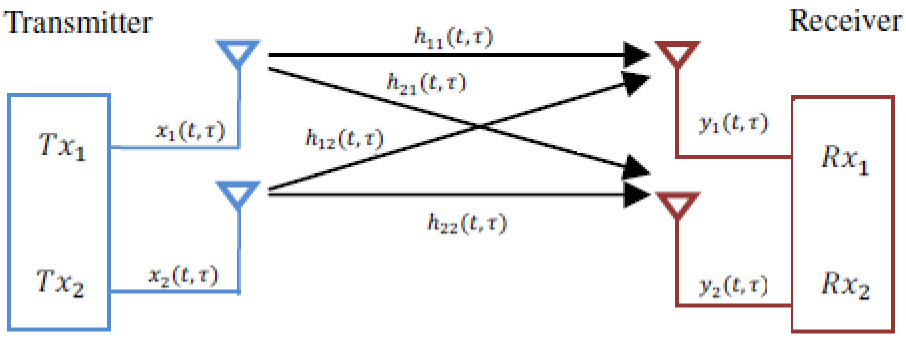

Fig. 2.4 – MIMO 2x2 channel configuration.

The drawbacks of MIMO is the higher complexity of the analog and digital domains. For point-to-point links, complexity at the receiver is usually a greater concern than transmitter's one. For example, the complexity of optimal signal detection alone grows exponentially with the number of transmitting antennas. In multiuser systems, complexity at the transmitter is also a concern since advanced coding schemes must often be used to transmit information simultaneously to more than one user while maintaining a low level of inter-user interference. This prohibitive complexity motivates a continuous search for computationally efficient, considering optimal or suboptimal detectors.

2.4 Massive MIMO

Massive MIMO is an emerging technology that scales up MIMO by several orders of magnitude compared to current state-of-the-art. With massive MIMO, we think of systems that use antenna arrays with a few hundred antennas, simultaneously serving many tens of mobile terminals at the same time-frequency resource. For example, a base station (BS) equipped with an array of M active antenna elements, using these to communicate with K single-antenna (or not) terminals.

The basic premise behind massive MIMO is to reap all the benefits of conventional MIMO, but on a much greater scale. The general multi-user MIMO concept has been around for decades, but the vision of actually deploying BSs with more than a handful of service antennas is relatively new [15]. By doing a coherent processing of the signals over the array, a transmit precoding can be used in the downlink to focus each signal at its desired terminal, and receive combining can be used in the uplink to discriminate the signals sent from different terminals. In the downlink, this scheme would result in a set of directive beams as it's pictured in Fig. 2.5. Overall, massive MIMO is an enabler for the development of future broadband (fixed and mobile) networks which will be energy-efficient, secure, and robust, and will use the spectrum efficiently.

Many different configurations and deployment scenarios for the antenna arrays used by a massive MIMO system can be envisioned, as we can see at the example in Fig. 2.6. Each antenna unit would be small, and active, preferably fed via an optical or electric digital bus.

Massive MIMO scenario using beamforming

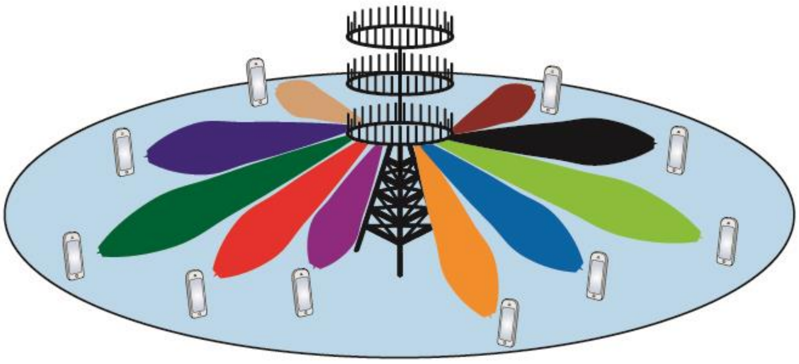

Fig. 2.5 - Massive MIMO scenario.

Massive MIMO relies on spatial multiplexing that depends on the base station's channel knowledge accuracy, both on the uplink and the downlink. On the uplink, this task can be easy to accomplish by having the terminals sending pilots. Then, combining these pilots and additional information that can be taken from data, base station estimates the channel responses to each of the terminals. The downlink case turns out to be more difficult. In conventional MIMO systems, like the LTE standard, the base station sends out pilot waveforms, based on which the mobile terminals estimate the channel responses and quantize the obtained estimates to then feed them back to the base station. This will not be feasible in massive MIMO systems, at least not when operating in a high-mobility environment, for two reasons:

- First, optimal downlink pilots should be mutually orthogonal between the antennas. This means that the amount of time-frequency resources needed for downlink pilots scales as the number of antennas, so a massive MIMO system would require up to a hundred times more such resources than a conventional system;

Possible massive MIMO antenna configuration

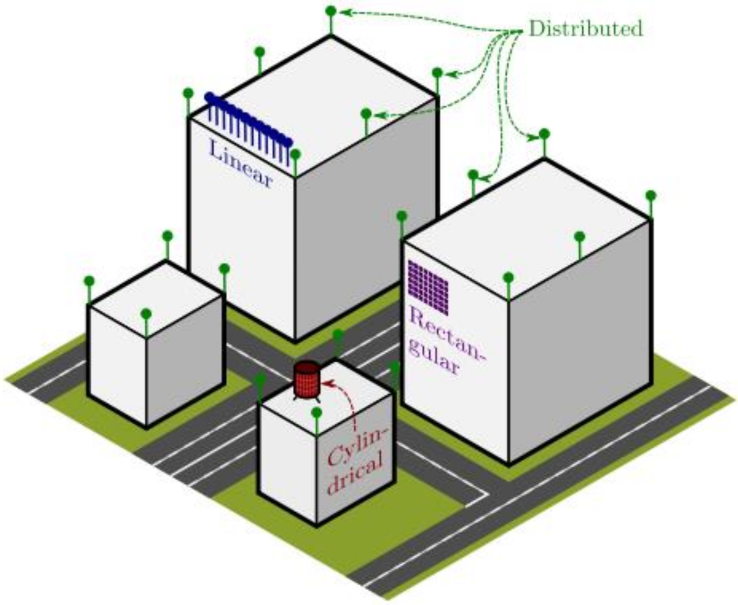

Fig. 2.6 - Possible antenna configurations and deployment scenarios for a massive MIMO base station.

- Second, the number of channel responses that each terminal must estimate is also proportional to the number of base station antennas. Hence, the uplink resources needed to inform the base station about the channel responses would be up to a hundred times larger than in conventional systems. Generally, the solution is to operate in TDD mode, and rely on reciprocity between the uplink and downlink channels [14].

The canonical massive MIMO system operates in TDD mode, where uplink and downlink transmissions take place in the same frequency resource but are separated in time. The physical propagation channels are reciprocal—meaning that the channel responses are the same in both directions—which can be utilized in TDD operation. In particular, massive MIMO systems exploit the reciprocity to estimate the channel responses on the uplink and then use the acquired channel state information (CSI) for both uplink receive combining and downlink transmit precoding of payload data.

Since the transceiver hardware is generally not reciprocal, calibration is needed to exploit the channel reciprocity in practice. Fortunately, the uplink-downlink hardware mismatches only change by a few degrees over a one-hour period and can be mitigated by simple relative calibration methods, even without extra reference transceivers and by only relying on mutual coupling between antennas in the array [16].

There are several good reasons to operate in TDD mode. Firstly, only the BS needs to know the channels to process the antennas' signals coherently. Secondly, the uplink estimation overhead is proportional to the number of terminals, but independent of M. This makes the protocol fully scalable with respect to the number of service antennas. Furthermore, basic estimation theory tells us that the estimation quality (per antenna) is not reduced by adding more antennas at the BS. In fact, the estimation quality improves with M if there is a known correlation structure between the channel responses over the array [3].

Since fading makes the channel responses vary over time and frequency, the estimation and payload transmission must fit into a time/frequency block where the channels are approximately static. The dimensions of this block are given by the coherence bandwidth Bc Hz and the coherence time Tc s, which fit $\tau = BcTc$ transmission symbols. Massive MIMO can be implemented either using single-carrier or multi-carrier modulation.

2.5 SC-FDE

Despite the success of OFDM, this approach suffers from well-known drawbacks such as a large PAPR (Peak-to-Average Power Ratio), intolerance to amplifier nonlinearities, and high sensitivity to carrier frequency offsets. An alternative low-complexity approach to mitigate ISI is the use of FDEs (Frequency Domain Equalizers) in SC (Single Carrier) communications.

Systems employing FDE are closely related to OFDM systems. In fact, in both cases digital transmission is carried out blockwise, and relies on FFT/IFFT operations. Therefore, SC systems employing FDE enjoy a similar complexity to OFDM systems with the advantages of not having the stringent requirements of highly accurate frequency synchronization and linear power amplification as in OFDM, which can leverage the usage of cheaper components in user terminals with a high efficiency. The substantial lower computational complexity of FDEs compared to their TD (Time Domain) equalization counterparts is also worth to mention.

The overall SC-FDE receiver structure is ilustrated in Fig. 2.7.

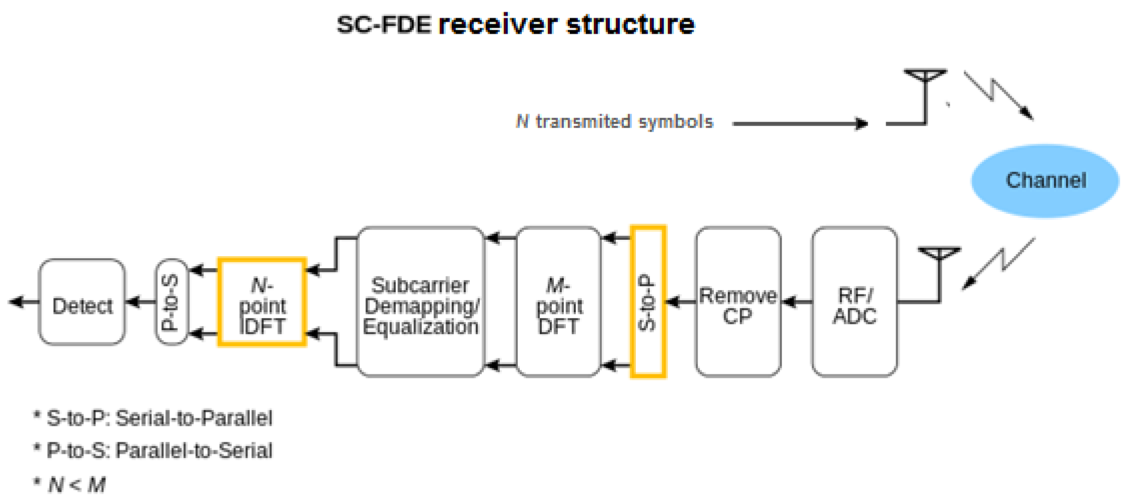

Fig. 2.7 – SC-FDE Receiver structure [17] adapted.

The first proposal of SC-FDE (Single Carrier Frequency-Domain Equalization) in digital communication systems dates back to 1973 [18].

Block transmission techniques, with appropriate cyclic prefixes and employing FDE techniques, have been shown to be suitable for high data rate transmission over severely time-dispersive channels [19]. Two possible alternatives based on this principle are OFDM and SC modulation using FDE (or SC-FDE). Due to the lower envelope fluctuations of the transmitted signals and, implicitly a lower PAPR (Peak-to-Average Power Ratio), SC-FDE schemes are especially interesting for the uplink transmission (i.e., the transmission from the mobile terminal to the base station), being considered for use in the upcoming LTE cellular system.

As we can observe in Fig. 2.8, SC-FDE is a modulation where each symbol occupies the total band allocated for the channel, so that the symbol's energy is distributed along the transmission band. The complex envelope of an N-symbol block (assuming that N is even) can be written as

$$s(t) = \sum_{n=-\frac{N}{2}}^{\frac{N}{2}-1} s_n r(t - nT_s)\,, \tag{2.1}$$

where $r(t)$ represents the transmitted impulse, T_s is the symbol duration in seconds and s_n is a complex coefficient representing the n^{th} symbol resulting from a direct mapping rule of the original data bits into a selected signal constellation – in the case of this thesis, the applied modulation is QPSK (Quadrature Phase Shift Keying).

OFDM vs SC-FDE frequency usage

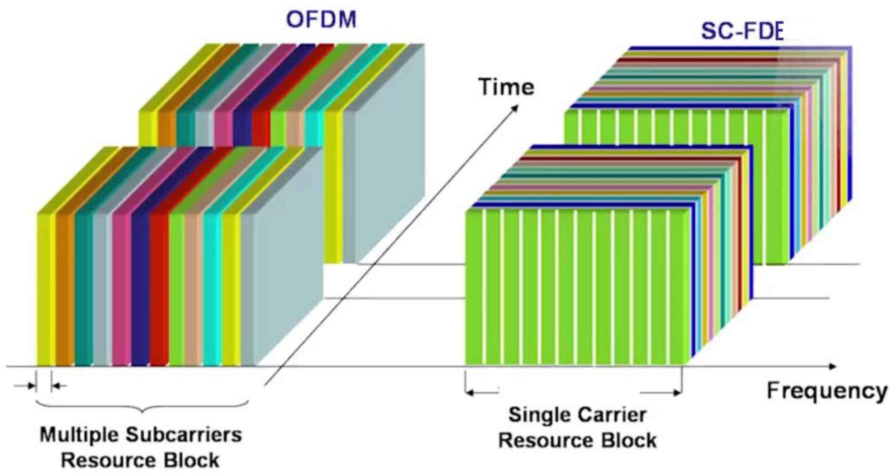

Fig. 2.8- OFDM vs SC-FDE [20] adapted.

If we apply the Fourier Transformation (FT) to both sides of the previous expression we obtain the frequency-domain equivalent of the signal

$$S(f) = \mathfrak{F}\{s(t)\} = \sum_{n=-\frac{N}{2}}^{\frac{N}{2}-1} s_n R(f) exp(-j2\pi f n T_s) \,, \tag{2.2}$$

where $R(f)$ represents the FT of $r(t)$. We can easily conclude that the transmission band associated to each symbol s_n is the band occupied by $R(f)$.

The SC-FDE receiver can be easily extended to an L-branch diversity scenario. In this case, the frequency-domain samples at the FDE's output are given by

$$\tilde{S}_k = \sum_{l=1}^{L} F_k^{(l)} Y_k^{(l)} \,, \tag{2.3}$$

where the set $\left\{F_k^{(l)}\,;\, \mathrm{k} = 0, 1, \dots, N-1\right\}$ $(l = 1, .., L)$ is established dependent on the used algorithm.

2.6 Precoding

Precoding is a generalization of beamforming to support multi-stream (or multi-layer) transmission in multi-antenna wireless communications. In conventional single-stream beamforming, when the receiver has just one antenna, the same signal is transmitted by each of the transmit antennas with appropriate weighting (phase and gain) such that the signal power is maximized at the receiver output. When the receiver has multiple antennas, single-stream beamforming cannot simultaneously maximize the signal level at all of the receive antennas. In order to maximize the throughput in multiple receive antenna systems, multi-stream transmission is generally required.

In point-to-point systems, precoding means that multiple data streams are sent by the transmit antennas with independent and appropriate weightings such that the link throughput is maximized at the receiver output. In multi-user MIMO, the data streams are intended for different users (known as SDMA) and some measure of the total throughput (e.g., the sum performance or max-min fairness) is maximized. In point-to-point systems, some of the benefits of precoding can be realized without requiring channel state information at the transmitter, while such information is essential to handle the inter-user interference in multi-user systems.

2.6.1 Precoding technique

Precoding exploits transmit diversity by weighting the information streams, i.e. the transmitter sends the precoded information to the receiver considering the pre-knowledge of the channel. The receiver is a simple detector, such as a matched filter, and does not have to know the channel side information. This technique will reduce the corrupted effect of the communication channel. For instance, when information $\boldsymbol{S}$ is sent, it passes through the channel $\boldsymbol{H}$ and Gaussian noise, $\boldsymbol{N}$, is added. The received signal at the receiver front-end will be

$$\boldsymbol{R} = \boldsymbol{S}\boldsymbol{H} + \boldsymbol{N}. \tag{2.4}$$

The receiver must know the information about $\boldsymbol{H}$ and $\boldsymbol{N}$, and can suppress the effect of $\boldsymbol{N}$ by increasing SNR. The needs of information about the channel $\boldsymbol{H}$, known as CSI, at the receiver, will increase the complexity. The receiver UE (User Equipment) has to be simple for many reasons, like cost or size of it. So, in order to mitigate this complexity, the transmitter (base station) will do the hard work and do the channel estimation.

Let's call $\boldsymbol{H}_{est}$ the estimated channel, hence for a system with precoder the information will be coded as

$$\frac{\boldsymbol{S}}{\boldsymbol{H}_{est}}. \tag{2.5}$$

The received signal will be

$$\boldsymbol{R} = \left(\frac{\boldsymbol{H}}{\boldsymbol{H}_{est}}\right)\boldsymbol{S} + \boldsymbol{N}. \tag{2.6}$$

If the estimation is perfect, $\boldsymbol{H}_{est} = \boldsymbol{H}$ and $\boldsymbol{R} = \boldsymbol{S} + \boldsymbol{N}$.

The name of this method is "precoding" because it's a preprocessing technique that uses transmit diversity and it is similar to equalization, however, it's done in the transmitter side. The channel equalization performed by precoder aims to minimize channel errors, but the precoder aims to minimize the error in the receiver output.

2.6.2 Precoding for Multi-user MIMO Systems

In multi-user MIMO, a multi-antenna transmitter communicates simultaneously with multiple receivers (each having one or multiple antennas). This is known as space-division multiple access (SDMA). From an implementation perspective, precoding algorithms for SDMA systems can be sub-divided into linear and nonlinear precoding types.

The capacity achieving algorithms are nonlinear, but linear precoding usually attains reasonable performance with much lower complexity. Linear precoding strategies include maximum ratio transmission (MRT) and zero-forcing (ZF) precoding. There are also precoding strategies tailored for low-rate feedback of CSI, for example random beamforming. Nonlinear precoding is designed based on the concept of dirty paper coding (DPC), which shows that any known interference at the transmitter can be subtracted without the penalty of radio resources if the optimal precoding scheme can be applied on the transmit signal [6].

In point-to-point MIMO, performance maximization has a clear interpretation and objective, however a multi-user system cannot simultaneously maximize the performance for all users. This can be regarded as a multi-objective optimization problem where each objective corresponds to maximization of the capacity of each user. The usual way to simplify this problem is to select a system utility function; for example, the weighted sum capacity where the weights correspond to the system's subjective user priorities. Furthermore, there might be more users than data streams, requiring a scheduling algorithm to decide which users to serve at a given time instant. As an example of the precoding usage, we can have beamforming, as the exemplified in Fig. 2.9, where the same signal is emitted from each of the transmit antennas with appropriate weighting (phase and gain) and these parameters are adjusted in such way that the signal power is maximized at the receiver output (add up constructively).

Typical transmission vs Transmission using beamforming

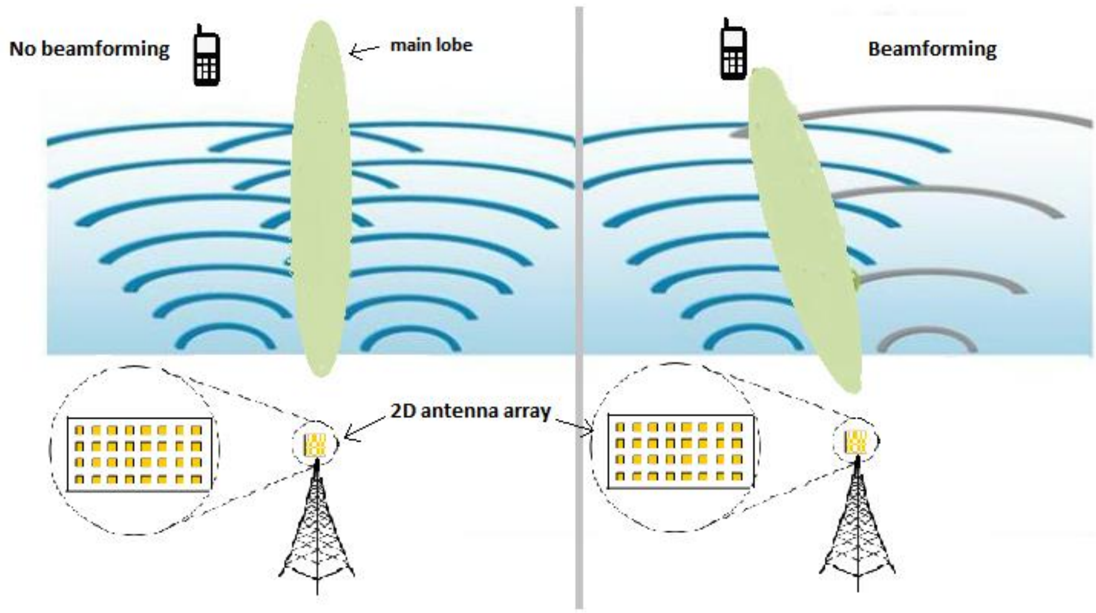

Fig 2.9 – Typical transmission waves vs Beamforming waves.

2.7 Scenario characterization

The scenario depicted in this thesis was based on state of the art technology. The massive MIMO uplink communication scheme scenario is analyzed and simulated. We consider the multi-user massive MIMO scenario similar to the one pictured in Fig. 2.10, which characterizes the up-link transmission between T single-antenna MT (Mobile Transceiver) and a BS (Base Station) with R receiving antennas, where R >> T (the generalization for the case where we have multiple antennas at the MTs is straightforward). Data blocks with N =256 QPSK (Quaternary Phase Shift Keying) data symbols are adopted as transmission blocks.

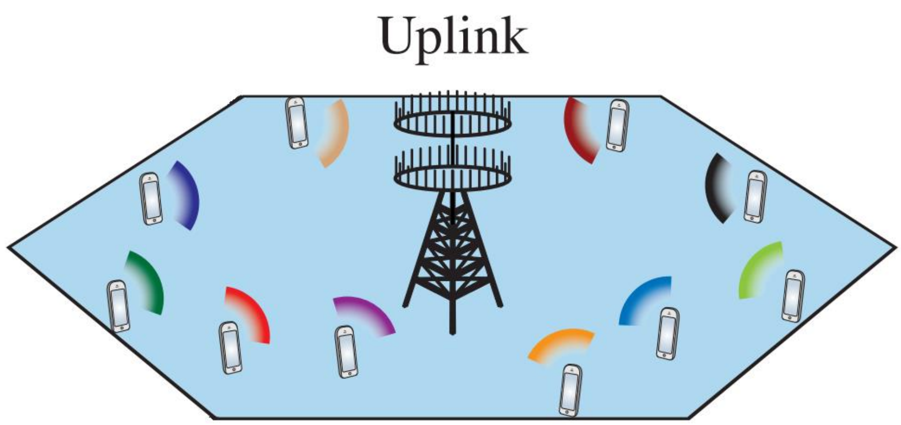

Fig. 2.10– Massive MIMO up-link scenario.

The channels between each transmit and receive antenna are assumed to be severely time-dispersive and an SC-FDE transmission technique is employed by each MT combined with a QPSK modulation. The t*th* MT transmits the block of N data symbols

$$x_n^{(t)}; n = 0,1, \dots, N-1. \tag{2.7}$$

As with other SC-FDE schemes, an appropriate cyclic prefix is appended to each transmitted block and removed at the receiver. The resulting signal is serie-to-paralel converted and the CP samples are removed, leading to the received time-domain samples, so the received block at the r*th* antenna of the BS is

$$y_k^{(r)}; k = 0,1, \dots, N-1. \tag{2.8}$$

If appropriate cyclic prefixes were employed, these samples are passed to the frequency-domain by an N-point DFT, leading to the corresponding frequency-domain block

$$\boldsymbol{Y}_k^{(r)}; k = 0,1, \dots, N-1, \tag{2.9}$$

which satisfies

$$\boldsymbol{Y}_k = [y_k^{(1)}, \dots, y_k^{(R)}]^T = \boldsymbol{H}_k \boldsymbol{X}_k + \boldsymbol{N}_k, \tag{2.10}$$

where $\boldsymbol{H}_k$ denotes the $R\ x\ T$ channel matrix for the kth frequency, with (r,t)*th* element $\boldsymbol{H}_k^{(r,t)}$, $\boldsymbol{X}_k = [X_k^{(1)}, \dots, X_k^{(T)}]^T$, and $\boldsymbol{N}_k$ denotes the channel noise.

For a linear MMSE-based receiver the data symbols can be obtained from the IDFT of the block $\{\tilde{X}_k^{(t)}; k = 0,1, \dots, N-1\}$, by

$$\tilde{X}_k = [X_k^{(1)}, \dots, X_k^{(R)}]^T = (\boldsymbol{H}_k \boldsymbol{H}_k^H + \alpha \mathbf{I})^{-1}\ \boldsymbol{H}_k^H . \boldsymbol{X}_k, \tag{2.11}$$

where $\mathbf{I}$ is an appropriate identity matrix and $\alpha = E\left[\left|\boldsymbol{N}_k^{(r)}\right|^2\right]/E[\left|\boldsymbol{X}_k^{(t)}\right|^2]$ is assumed identical for all values of t and r. However, this involves the inversion of a matrix for each frequency, and the dimensions of these matrices can be very high in massive MIMO systems.

Massive MIMO schemes usually employ simpler receivers. The most popular are probably the ones based on the MRC. These receivers take advantage of the fact that

$$\boldsymbol{H}_k^H \boldsymbol{H}_k \approx R\mathbf{I} \,, \tag{2.12}$$

is an approximation that is accurate when $R >> 1$ (i.e., for massive MIMO systems), provided that the channels between different transmit and receive antennas have small correlation [21]. For SC-FDE we could employ a frequency-domain receiver with MRC at each frequency, based on $\boldsymbol{H}_k^H \boldsymbol{Y}_k$. However, the residual interference levels can still be substantial, especially for moderate values of R/T. In this system, it is assumed that all the packets associated to each uplink transmission have the same duration, which corresponds to a FFT block. Perfect channel estimation and synchronization between local oscillators is also assumed. A cyclic prefix of different length is added to each FFT block to compensate the different propagation delays, so it is assumed that colliding packets arrive simultaneously. In every simulation of this chapter it is admitted that all the UEs transmit with the same power and that every UE present in the network has always a packet to transmit.

Multiple UEs can transmit in the same time slot to the same BS and more transmissions of the same uplink signal can be used to enhance the reception.

2.7.1 Channel models

Channel models have a very important role in the performed simulations since they define how the channel responds to the transmitted signal. Two types of models were used to simulate the channel's behavior:

The first channel model is denominated by 'XTAP'. In order to simulate the effects of multipath fading, the model created consists of a delay line with several taps. In this context, a tap is just a point on the delay timeline that corresponds to a certain value of delay. The signals from each tap can be "summed" and then the composite signal represents what a real radio wave might look like as received. This signal is subject to multipath fading, having a Rayleigh fading for each path (16 paths were considered between each communicating antennas). The summing referred above is the mixing of the individual signals from the various taps. Important to remind that these can be summed together in different ways to simulate how time can play a part in the real mixing of the multipath signals.

The second model used is referred as 'CLUST'. The name is related with the antennas configuration as this model is based on clusters of antennas. Essentially, there are Ru groups of Rb antennas spaced by half of wavelength between antennas, and spacing between groups relatively high (in the order of ten wavelengths), which makes the correlation between groups to be very low, almost uncorrelated. Also this model takes into account that within these groups the channel are very similar, with exception of a $e^{j2\pi\frac{d}{\lambda}\cos(\theta)}$ factor (d is the scpacing between antennas of the same cluster and λ the wavelength) between antennas of the same group. This fact is the one which allows beamforming to happen. Also in this model there are clusters of rays that arrive to the receiver with little delays between them and this is represented by groups of arriving rays over time when we observe the impulsive response of each channel model.

3

Conventional detection schemes

In communications, the receiver often observes a superposition of separately transmitted information symbols. From the receiver's perspective, the problem is then to separate the transmitted symbols.

The most important and motivating application for the discussion here is receivers for multiple-antennas such as massive MIMO systems, where several transmit antennas can simultaneously send multiple data streams. Essentially the same problem occurs in systems where the channel itself introduces time or frequency dispersion, in multiuser detection, and in cancellation of crosstalk. When the signal is a combination of several waves, the total signal amplitude may experience deep fades over the time or space. The most popular way to combat this effect is to use some form of diversity combining. The presence of diversity also poses other interesting problem: how do we effectively use the information from all the antennas to demodulate the data?

This chapter starts with the explanation of the overall discrete-time model used, along with considered assumptions. It continues with the description of some basic combining algorithms as well as iterative algorithms using hard or soft decisions. The combinations of these techniques was the basis of the proposed receivers. The chapter finishes with the introduction and brief explanation of a technique that can be used in precoding and equalization, singular value decomposition, to improve the efficiency of these processes.

3.1 Overall Discrete-time Model

The overall channel and equalizer can be represented by a overall digital filter with impulse response

$$\boldsymbol{q} = (q_0, q_1, \ldots, q_{N+L-1})^T , \tag{3.1}$$

where

$$q_N = \sum_{j=0}^{N-1} w_j q_{n-j} = \mathbf{w}^T \boldsymbol{p}(n) , \tag{3.2}$$

with

$$p(n) = (p_n, p_{n-1}, p_{n-2}, \ldots, p_{n-N+1})^T , \tag{3.3}$$

and $p_i = 0, i < 0, i > L$. That is, $\mathbf{q}$ is the discrete convolution of $\mathbf{p}$ and $\mathbf{w}$.

We call $\mathbf{z}^H \boldsymbol{Hw}$ the effective channel. For optimum performance, $\mathbf{w}$ and $\mathbf{z}$ should be chosen as a function of the channel to minimize the probability of error.

We can also assume the following:

1. The channel is flat fading – In simple terms, it means that the multipath channel has only one tap. So, the convolution operation reduces to a simple multiplication;

2. The channel experience by each transmit antenna is independent from the channel experienced by other transmit antennas;

3. For the $\mathbf{t}\boldsymbol{th}$ transmit antenna to $\mathbf{r}\boldsymbol{th}$ receive antenna, each transmitted symbol gets multiplied by a randomly varying complex number $\boldsymbol{h}_{r,t}$. As the channel under consideration is a Rayleigh channel, the real and imaginary parts of $h_{r,t}$ are Gaussian distributed with mean $\boldsymbol{\mu}_{h_{r,t}} = \mathbf{0}$ and variance $\boldsymbol{\sigma}^2_{h_{r,t}} = \frac{1}{2}$;

4. The channel experienced between each transmit to the receive antenna is independent and randomly varying in time;

5. On the receive antenna, the noise $\boldsymbol{n}$ has the Gaussian probability density function given by

$$p(n) = \frac{1}{\sqrt{2\pi\sigma^2}} e^{\frac{-(n-\mu)^2}{2\sigma^2}} , \tag{3.4}$$

with $\boldsymbol{\mu} = \mathbf{0}$ and $\boldsymbol{\sigma}^2 = \frac{N_0}{2}$;

6. The channel $h_{r,t}$ is known at the receiver.

3.2 Basic combining algorithms

Some basic combining algorithms are:

- Switching;
- Selection;
- Zero forcing;
- Equal gain combining;
- Maximum ratio combining;
- Maximum minimum squared error.

These linear combining algorithms might be implemented as RF process (analog) or can be realized in the digital domain. In diversity combining algorithms the signal in each branch is multiplied by a diversity combining gain. The branches are also co-phased and then added. A typical receiver architecture with diversity combining is illustrated in Fig. 3.1.

Diversity combining receiver architecture

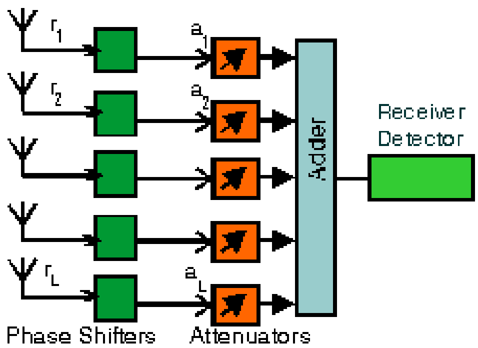

Fig. 3.1 – Example of diversity combining receiver architecture.

3.2.1 Switching

Switching algorithm consists in selecting the highest power gain branch. In Fig. 3.2 we can observe the signal envelope of a two antenna receiver using a switching algorithm. In this case, the transition between antennas is done immediately when a higher gain is detected. Fig. 3.3 shows a typical architecture of a receiver employing switching algorithm where a RSSI (Received Signal Strength Indicator) is used to make the gain comparison.

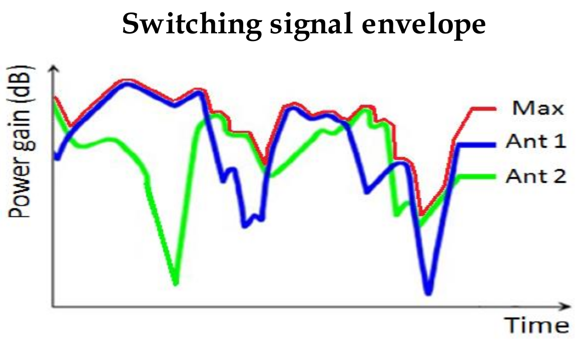

Fig. 3.2 – Example of switching algorithm signal envelope.

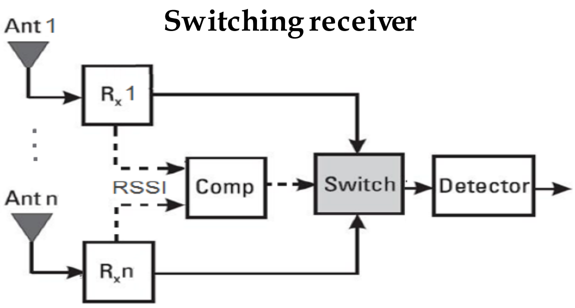

Fig. 3.3 – Example of switching algorithm receiver architecture.

3.2.2 Selection

In this algorithm, the selected branch is kept active without revision until it reaches a minimum threshold. Just at that point, the algorithm will switch to the maximum power gain antenna. Because in this process the branches' power gain is only evaluated when the current one falls below a given threshold, it can exist a very poor performance when the current branch has low power gain but still over the threshold, and at the same time there are other branches with much higher power gain. This is noticeable in Fig. 3.4 where we can observe a power gain envelope of a receiver using selection. In the next figure, 3.5, we can see a typical architecture of this algorithm.

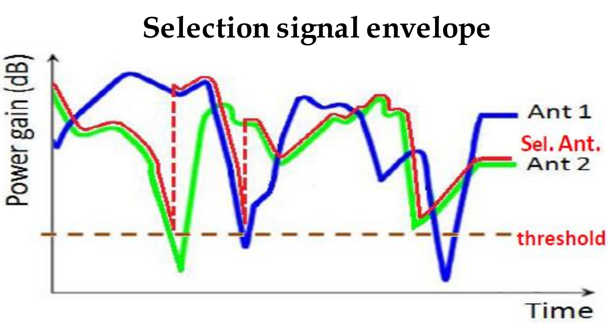

Fig. 3.4 – Example of selection algorithm signal envelope.

Selection receiver

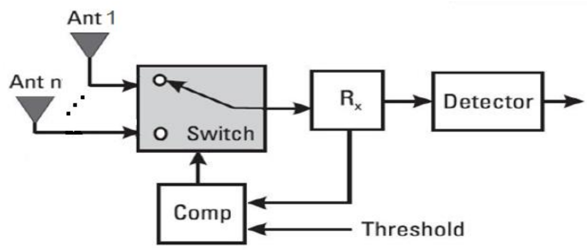

Fig. 3.5 – Example of selection algorithm receiver architecture.

3.2.3 Zero Forcing

The ZF detector considers the signal from each transmit antenna as the target signal and the rest of signals as interferers. The main goal of this detector is setting the interferers amplitude to zero and this is done by inverting the channel response and rounding the result to the closest symbol in the alphabet considered. Then the equation (2.10) is left multiplied by the inverse channel, $\boldsymbol{H^{-1}}$. However, when the channel matrix is tall (R>T), the pseudo inverse of $\boldsymbol{H}$ is then used, what leads to the following inversion step

$$\boldsymbol{W} = (\boldsymbol{H^H H})^{-1}\boldsymbol{H^H}. \tag{3.5}$$

This matrix is also known as the pseudo inverse for a general *m x n* matrix.

Let the component of $\mathbf{p}$ of greatest magnitude be denoted by $\boldsymbol{p_{d1}}$. Note that we may have $\boldsymbol{d_1} \neq 0$. Let the number of equalizer taps be equal to N = $2\boldsymbol{d_2} + 1$ where $\boldsymbol{d_2}$ is an integer. Perfect equalization means that

$$\boldsymbol{q} = \boldsymbol{e_d}(0,0,\ldots,0,1,0,\ldots,0,0)^T , \tag{3.6}$$

where *d* zeroes precede the "1" and *d* is an integer representing the overall delay, a parameter to be optimized. Unfortunately, perfect equalization is difficult to achieve and does not always yield the best performance.

With a ZF equalizer, the tap coefficients $\mathbf{w}$ are chosen to minimize the peak distortion of the equalized channel, defined as

$$D_p = \frac{1}{|q_d|} \sum_{\substack{n=0 \\ n \neq d}}^{N+L-1} |q_n - \hat{q}_n| , \tag{3.7}$$

where $\hat{q}_n = (\hat{q}_0, \ldots, \hat{q}_{N+L-1})^T$ is the desired equalized channel and the delay d is a positive integer chosen to have the value $d = d_1 + d_2$. Lucky showed that if the initial distortion without equalization is less than unity, i.e.,

$$D_p = \frac{1}{|p_{d_1}|} \sum_{\substack{n=0 \\ n \neq d_1}}^{L} |p_n| < 1\,, \tag{3.8}$$

then D_p is minimized by those N tap values which simultaneously cause $q_n = \hat{q}_j$ for $d - d_2 \leq j \leq d + d_2$. However, if the initial distortion before equalization is greater than unity, the ZF criterion is not guaranteed to minimize the peak distortion.

For the case when $\hat{q} = e_d^T$, the equalized channel is given by

$$\boldsymbol{q} \;=\; \left(q_0, \ldots, q_{d_1-1}, 0, \ldots, 0, 1, 0, \ldots, 0, q_{d_1+N}, \ldots, q_{N+L-1}\right)^T. \tag{3.9}$$

In this case the equalizer forces zeroes into the equalized channel and, hence, the name "zero-forcing equalizer". If the ZF equalizer has an infinite number of taps, it is possible to select the tap weights so that $D_p = 0$, i.e., $\boldsymbol{q} = \hat{\boldsymbol{q}}$. Assuming that $\hat{q}_n = \delta n_0$, this condition means that

$$\mathrm{Q(z)} = 1 = \mathrm{W(z)P(z)}. \tag{3.10}$$

Therefore, $W(z) = \frac{1}{\mathrm{P(z)}}$ and the ideal ZF equalizer has a discrete transfer function that is simply the inverse of overall channel P(z).

For a known channel impulse response, the tap gains of the ZF equalizer can be found by the direct solution of a simple set of linear equations. To do so, we form the matrix

$$\boldsymbol{P} = [p(d_1), \ldots, p(d), \ldots, p(N + d_1 - 1)]\,, \tag{3.11}$$

and the vector

$$\hat{\boldsymbol{q}} \;=\; (\hat{q}_{d1}, \ldots, \hat{q}_d, \ldots, \hat{q}_{N+d_1-1})^T\,. \tag{3.12}$$

Then the array of optimal tap gains, $\mathbf{w}_{\mathrm{op}}$, satisfies

$$\mathbf{w}_{\mathrm{op}}{}^T\mathbf{P} = \tilde{\boldsymbol{q}}^T \;\rightarrow\; \mathbf{w}_{\mathrm{op}} = (\mathbf{P}^{-1})^T\tilde{q}. \tag{3.13}$$

The ZF detector presents the problem of, in some cases, finding singular channel matrices that are not invertible. Another disadvantage is the fact that ZF focuses on cancelling completely the interference at the expense of not taking care of the noise.

3.2.4 Equal Gain Combining

While selection diversity combining is easily implemented, equal gain detection receivers have been shown to improve the average probability of symbol error performance [22]. Equal gain combiners require only moderate hardware complexity because each of the receive antennas weights is restricted to be of magnitude $\frac{1}{\sqrt{M_r}}$. On the $\boldsymbol{i}^{th}$ receive antenna, equalization is performed at the receiver by dividing the received symbol $\boldsymbol{y}_i$ by the apriori known phase of $\boldsymbol{h}_i$. The channel $\boldsymbol{h}_i$ is represented in polar form as $|\boldsymbol{h}_i|\boldsymbol{e}^{j\theta}$. The decoded symbol is the sum of the phase compensated channel from all the receive antennas.

The gain of the effective channel for an EGD system can be bounded by

$$|\boldsymbol{z}^H \boldsymbol{H}\boldsymbol{w}|^2 = \frac{1}{M_r}\left|\sum_{m=1}^{M_r} \boldsymbol{e}^{-j\phi_m}(\boldsymbol{H}\boldsymbol{w})_m\right|^2 \tag{3.14}$$

$$\leq \frac{1}{M_r}\left(\sum_{m=1}^{M_r} |(\boldsymbol{H}\boldsymbol{w})_m|\right)^2 \tag{3.15}$$

$$= \frac{1}{M_r}\|\boldsymbol{H}\boldsymbol{w}\|^2 , \tag{3.16}$$

where $(\boldsymbol{H}\boldsymbol{w})_m$ is the $\boldsymbol{m}^{th}$ entry of the array $\boldsymbol{H}\boldsymbol{w}$ and the inequality follows from the equal gain properties of **z**. The bound is achievable when

$$z = \frac{1}{M_r}\boldsymbol{e}^{j(\phi + phase(\boldsymbol{H}\boldsymbol{w}))} , \tag{3.17}$$

where $\boldsymbol{\phi}$ is an arbitrary phase angle. Using the optimal equal gain combining vector

$$\boldsymbol{\Gamma}_r = \frac{1}{M_r}\|\boldsymbol{H}\boldsymbol{w}\|^2 . \tag{3.18}$$

This can be rewritten for equal gain transmission as

$$\boldsymbol{\Gamma}_r = \frac{1}{M_r M_t} \left\| \boldsymbol{H} e^{j\theta} \right\|^2 . \tag{3.19}$$

Therefore, the optimal phase vector θ is given by

$$\theta \in \arg \max_{\vartheta \in [0,2\pi]^{M_t}} \left\| \boldsymbol{H} e^{j\vartheta} \right\| . \tag{3.20}$$

The optimization problem defined has no known simple, closed-form solution. Again note that the resolution defined also does not have a unique solution. In fact, if $\frac{1}{M_t} e^{j\vartheta}$ is an optimal equal gain transmission vector then $\frac{1}{M_t} e^{j\xi} e^{j\vartheta}$ is also optimal for any $\xi \in [0, 2\pi]$ because $\left\| \boldsymbol{H} e^{j\theta} \right\|^2 = \left\| \boldsymbol{H} e^{j\xi} e^{j\theta} \right\|^2$.

3.2.5 Maximum Ratio Combining

Maximum ratio detection provides the best performance among all combining schemes thanks to the absence of constraints placed on the set of possible combining vectors. Although it's similar to EGC algorithm, the combining vector in MRC is designed specifically to maximize the effective channel gain $|\boldsymbol{z}^H \boldsymbol{H} \boldsymbol{w}|^2$. For MRC receiver, the effective channel gain can be upper bounded by

$$|\boldsymbol{z}^H \boldsymbol{H} \boldsymbol{w}|^2 \leq \|\boldsymbol{z}^H\|^2 \|\boldsymbol{H} \boldsymbol{w}\|^2 = \|\boldsymbol{H} \boldsymbol{w}\|^2 . \tag{3.21}$$

This upper bound is achievable if

$$\boldsymbol{z} = \frac{\boldsymbol{H} \boldsymbol{w}}{\|\boldsymbol{H} \boldsymbol{w}\|} . \tag{3.22}$$

Thus the optimum phase vector θ solves

$$\theta \in \arg \max_{\vartheta \in [0,2\pi]^{M_t}} \left\| \boldsymbol{H} e^{j\vartheta} \right\| . \tag{3.23}$$

Once again the phase vector $\boldsymbol{\theta}$ is not unique because $\mathbf{w}$ can be arbitrarily multiplied by any unit gain of the form $e^{j\xi}$ with $\xi \in [0, 2\pi]$.

3.3 Minimum Mean Squared Error

Let us consider a 2x2 MIMO system using MMSE detection. This scenario is illustrated in Fig. 2.4, in previous section. Let us now try to understand the math for extracting the two symbols which interfered with each other. In the first time slot, the received signal on the first receive antenna is,

$$Y_1 = H_{1,1}X_1 + H_{1,2}X_2 + N_1 = \begin{bmatrix} H_{1,1} & H_{1,2} \end{bmatrix} \begin{bmatrix} X_1 \\ X_2 \end{bmatrix} + N_1 \,. \tag{3.24}$$

The received signal on the second receive antenna is,

$$Y_2 = H_{2,1}X_1 + H_{2,2}X_2 + N_2 = \begin{bmatrix} H_{2,1} & H_{2,2} \end{bmatrix} \begin{bmatrix} X_1 \\ X_2 \end{bmatrix} + N_2 \,, \tag{3.25}$$

where Y_1, Y_2 are the received symbol on the first and second antenna respectively, $H_{i,j}$ is the channel from i^{th} transmit antenna to j^{th} receive antenna, X_1, X_2 are the transmitted symbols and N_1,N_2 is the noise on 1^{st},2^{st} receive antennas. We assume that the receiver knows $H_{1,1}$, $H_{1,2}$,$H_{2,1}$ and $H_{2,2}$. The receiver also knows Y_1 and Y_2. For convenience, the above equation can be represented in matrix notation as follows:

$$\begin{bmatrix} Y_1 \\ Y_2 \end{bmatrix} = \begin{bmatrix} H_{1,1} & H_{1,2} \\ H_{2,1} & H_{2,2} \end{bmatrix} \begin{bmatrix} X_1 \\ X_2 \end{bmatrix} + \begin{bmatrix} N_1 \\ N_2 \end{bmatrix}. \tag{3.26}$$

Equivalently,

$$\boldsymbol{Y} = \boldsymbol{HX} + \boldsymbol{N}. \tag{3.27}$$

The **MMSE** approach tries to find a coefficient $\boldsymbol{W}$ which minimizes the criterion,

$$E\{[\boldsymbol{W}Y - X][\boldsymbol{W}Y - X]^H\}\,, \tag{3.28}$$

solving,

$$\boldsymbol{W} = [\boldsymbol{H^H H} + \boldsymbol{N_0 I}]^{-1}\boldsymbol{H^H}. \tag{3.29}$$

When comparing to the equation in Zero Forcing equalizer, apart from the $\boldsymbol{N_0 I}$ term both the equations are comparable. In fact, when the noise term is zero, the MMSE equalizer reduces to a ZF equalizer.

Clearly, with ZF criterion the channel is completely inverted, resulting in a perfect equalized channel after the FDE, while MMSE criterion leads to an imperfect channel equalization. However, ZF criterion significantly enhances the channel noise at sub-channels with local deep notches, while with the MMSE criterion the noise-dependent term in the equation avoids noise enhancement effects for very low values of the local channel frequency response. As a result, the performance is dependent on the presence of noise.

In many real-time application, observational data is not available in a single batch. Instead the observations are made in a sequence. A naive application of previous formulas would have us discard an old estimate and re-compute a new estimate as fresh data is made available. But then we lose all information provided by the old observation. When the observations are scalar quantities, one possible way of avoiding such re-computation is to first concatenate the entire sequence of observations and then apply the standard estimation formula. This can be very tedious because as the number of observation increases so does the size of the matrices that need to be inverted and multiplied grow. Also, this method is difficult to extend to the case of vector observations.

Another approach to estimation from sequential observations is to simply update an old estimate as additional data becomes available, leading to finer estimates. Thus a recursive method is desired where the new measurements can modify the old estimates.

3.4 Iterative Block Decision Feedback Equalizer (IB-DFE)

Even though the performance of nonlinear receivers is better than the linear receivers, the first mentioned suffer from error propagation, especially for long feedback filters. To reduce error propagation, a promising IFDE (Iterative FDE) technique for SC-FDE, denoted IB-DFE (Iterative Block Decision Feedback Equalizer), was proposed in [23]. This technique was later extended to diversity scenarios and layered space-time schemes [24].

These IFDE receivers can be regarded as iterative DFE receivers with the feed-forward and the feedback operations implemented in the frequency domain. Since the feedback loop takes into account not just the hard decisions for each block but also the overall block reliability, error propagation is reduced.

Consequently, IFDE techniques offer much better performance than non-iterative methods [22, 23]. Within these IFDE receivers the equalization and channel decoding procedures are performed separately (i.e., the feedback loop uses the equalizer outputs instead of the channel decoder outputs). However, it is known that higher performance gains can be achieved if these procedures are performed jointly. This can be done by employing turbo equalization schemes, where the equalization and decoding procedures are repeated in an iterative way, being essential in MIMO schemes with high order modulations. Although initially proposed for time-domain receivers, turbo equalizers also allow frequency-domain implementations.

In order for the above schemes to operate correctly, good channel estimates are required at the receiver. Typically, these channel estimates are obtained with the help of pilot/training symbols that are multiplexed with the data symbols, either in the time domain or in the frequency domain.

In the case of MIMO or massive MIMO, where there is a R order space diversity, IB-DFE receiver is considered, for the ith iteration, to have the frequency-domain block at the output of the equalizer

$$\{\tilde{S}_k^{(i)}; k = 0,1, \dots, N-1\}, \tag{3.30}$$

with

$$\tilde{S}_k^{(i)} = \sum_{l=1}^{N_{Rx}} F_k^{(l,i)} Y_k^{(l)} - B_k^{(i)} \hat{S}_k^{(i-1)}, \tag{3.31}$$

where

$$\{F_k^{(l,i)}; k = 0,1, \dots, N-1\}, \tag{3.32}$$

are the feedforward coefficients associated to the lth diversity antenna and

$$\{B_k^{(i)}; k = 0,1, \dots, N-1\}, \tag{3.33}$$

are the feedback coefficients.

$\left\{\hat{S}_k^{(i-1)}; k = 0,1, \dots, N-1\right\}$ is the DFT of the block $\{\hat{s}_k^{(i-1)}; k = 0,1, \dots, N-1\}$, with $\hat{s}_n$ denoting "hard decision" of s_n from the previous FDE iteration.

Considering an IB-DFE with "hard decisions", it can be shown that the optimum coefficients F_k and B_k that maximize the overall SNR, associated to the samples $\tilde{S}_k$, are

$$B_k^{(i)} = \rho \left(\sum_{l=1}^{N_{Rx}} F_k^{(l,i)} H_k^{(l)} - 1 \right), \tag{3.34}$$

and

$$F_k^{(i)} = \frac{k H_k^{(l)*}}{\propto + (1 - (\rho^{(i-1)})^2) \sum_{l=1}^{N_{Rx}} \left| H_k^{(l\prime)} \right|^2}, \tag{3.35}$$

where $\boldsymbol{\rho}$ denotes the so called correlation factor,

$$\alpha = \frac{E\left[\left| N_k^{(l)} \right|^2 \right]}{E[|S_k|^2]}, \tag{3.36}$$

(which is common to all data blocks and diversity branches), and $\boldsymbol{k}$ is selected to guarantee that

$$\frac{1}{N} \sum_{k=0}^{N-1} \sum_{l=1}^{N_{Rx}} F_k^{(l,i)} H_k^{(l)} = 1 . \tag{3.37}$$

It can be seen from the previous expressions, that the correlation factor $\rho^{(i-1)}$ is a key parameter for the good performance of IB-DFE receivers, since it gives reliability in a block basis by measure of the estimates employed in the feedback loop (associated to the previous iteration). This is done in the feedback loop by taking into account the hard decisions for each block plus the overall block reliability, which reduces error propagation problems. The correlation factor $\rho^{(i-1)}$ is defined as

$$\rho^{(i-1)} = \frac{E[\hat{s}_n^{(i-1)} s_n^*]}{E[|s_n|^2]} = \frac{E[\hat{S}_k^{(i-1)} S_k^*]}{E[|S_k|^2]}, \tag{3.38}$$

where the block $\{\hat{s}_n^{(i-1)}; n = 0,1, \dots, N-1\}$ denotes the data estimates associated to the previous iteration, i.e., the hard decisions associated to the time-domain block at the output of the FDE,

$$\left\{ \bar{s}_n^{(i-1)}; n = 0,1, \dots, N-1 \right\} = IDFT\left\{ \hat{s}_n^{(i-1)}; n = 0,1, \dots, N-1 \right\}. \tag{3.39}$$

For the first iteration, no information exists about s_n, which means that $\rho = 0, B_k^{(0)} = 0$ and $F_k^{(i)}$ coefficients are given by

$$F_k = \frac{H_k^*}{\alpha + |H_k|^2}, \tag{3.40}$$

(in this situation the IB-DFE receiver is reduced to a linear FDE).

After the first iteration, the feedback coefficients can be applied to reduce a major part of the residual interference (considering that the residual Bit Error Rate (BER) does not assume a high value). After several iterations and for a moderate-to-high SNR, the correlation coefficient will be $\rho \approx 1$ and the residual ISI will be almost totally canceled.

3.4.1 IB-DFE with Soft Decisions

To improve the IB-DFE performance we took advantage of the usage of "soft decisions", $\bar{s}_n^{(i-1)}$, instead of "hard decisions", $\hat{s}_n^{(i-1)}$. In this way, the "blockwise average" is replaced by "symbol averages". This can be done by using

$$\left\{\bar{S}_{k,symbol}^{(i-1)}; k = 0,1, \dots, N-1\right\} = DFT\left\{\bar{s}_{n,symbol}^{(i-1)}; n = 0,1, \dots, N-1\right\}, \tag{3.41}$$

instead of

$$\left\{\bar{S}_{k,block}^{(i-1)}; k = 0,1, \dots, N-1\right\} = DFT\left\{\bar{s}_{n,block}^{(i-1)}; n = 0,1, \dots, N-1\right\}, \tag{3.42}$$

where $\bar{s}_{n,symbol}^{(i-1)}$ denotes the average symbol values conditioned to the FDE output from previous iteration, $\bar{s}_n^{(i-1)}$. To simplify the notation, $\bar{s}_{n,symbol}^{(i-1)}$ is replaced by $\bar{s}_n^{(i-1)}$ in the following equations.

For QPSK constellations, the conditional expectations associated to the data symbols for the i*th* iteration are given by

$$\bar{s}_n^{(i)} = \tanh\left(\frac{L_n^{I(i)}}{2}\right) + j\tanh\left(\frac{L_n^{Q(i)}}{2}\right) = \rho_n^I \hat{s}_n^I + j\,\rho_n^Q \hat{s}_n^Q, \tag{3.43}$$

with the LLRs (Log-Likelihood Ratio) of the "in-phase bit" and the "quadrature bit", associated to s_n^I and s_n^Q, given by

$$\mathrm{L}_n^{I(i)} = \frac{2}{\sigma_i^2}\tilde{s}_n^{I(i)}, \tag{3.44}$$

and

$$\mathrm{L}_n^{Q(i)} = \frac{2}{\sigma_i^2}\tilde{s}_n^{Q(i)}, \tag{3.45}$$

respectively, with

$$\sigma_i^2 = \frac{1}{2}E\left[\left|s_n - \tilde{s}_n^{(i)}\right|^2\right] \approx \frac{1}{2N}\sum_{n=0}^{N-1}\left|\hat{s}_n^{(i)} - \tilde{s}_n^{(i)}\right|^2, \tag{3.46}$$

where the signs of L_n^I and L_n^Q define the hard decisions $\hat{s}_n^I = \mp 1$ and $\hat{s}_n^Q = \mp 1$. In the expression of $\bar{s}_n^{(i)}$, the reliabilities of the "in-phase bit" and the "quadrature bit" of the n*th* symbols are denoted by ρ_n^I and ρ_n^Q, given by

$$\rho_n^{I(i)} = \frac{E[s_n^I \hat{s}_n^I]}{E[|s_n^I|^2]} = \left|\tanh\left(\frac{L_n^{I(i)}}{2}\right)\right|, \quad \rho_n^{Q(i)} = \frac{E[s_n^Q \hat{s}_n^Q]}{E\left[\left|s_n^Q\right|^2\right]} = \left|\tanh\left(\frac{L_n^{Q(i)}}{2}\right)\right|. \tag{3.47}$$

Therefore, the correlation coefficient employed in the feedforward coefficients will be given by

$$\rho^{(i)} = \frac{1}{2N}\sum_{n=0}^{N-1}\left(\rho_n^{I(i)} + \rho_n^{Q(i)}\right), \tag{3.48}$$

Obviously, for the first iteration $\rho_n^{I(i)} = \rho_n^{I(i)} = 0$ and, consequently, $\bar{s} = 0$. Therefore, the receiver with "blockwise reliabilities" (hard decisions), and the receiver with "symbol reliabilities" (soft decisions), employ the same feedforward coefficients; however, in the first the feedback loop uses the "hard-decisions" on each data block, weighted by a common reliability factor, whereas in the second the reliability factor changes from bit to bit.

The IB-DFE receiver can be implemented in two different ways, depending whether the channel decoding output is outside or inside the feedback loop. In the first case the channel decoding is not performed in the feedback loop, and this receiver can be regarded as a low complexity turbo equalizer implemented in the frequency domain. Since this is not a true “turbo" scheme, we will call it “Conventional IB-DFE". In the second case the IB-DFE can be regarded as a turbo equalizer implemented in the frequency domain and therefore we will denote it as “Turbo IB-DFE". For uncoded scenarios like the one we deal with, it only makes sense to employ conventional IB-DFE schemes. However, it is important to point out that in coded scenarios we could still employ a “Conventional IB-DFE" and perform the channel decoding procedure after all the iterations of the IB-DFE.

3.5 Singular Value Decomposition (SVD)

The MMSE receiver is known to be optimal only for an orthogonal channel, that is, when the matrix $\boldsymbol{H}$ has full rank and all its eigenvalues are equal. In general, the optimal MIMO receiver requires computationally intensive nonlinear operation such as maximum likelihood (ML) decoding (e.g., exhaustive search over all possible transmitted symbol vectors). However, if the channel is known at the transmitter (closed loop), the performance of the receiver can be improved by diagonalizing the channel with precoding at the transmitter.

Applications of precoding schemes, which are based on Singular Value Decomposition (SVD) of the channel matrix $\boldsymbol{H}$ assume almost always ideal channel knowledge at the transmitter and/or receiver site. In any case the MIMO channel matrix $\boldsymbol{H}$ is decomposed into eigenvalues. In case of an ideal radio channel knowledge the SVD based precoding procedure, which is applied at the transmitter site, is going to consider all possible eigenvalues which results in a perfect separation of all signals at the receive antenna output and into a minimum bit-error-rate (BER).

SVD can be looked at from three mutually compatible points of view. On the one hand, we can see it as a method for transforming correlated variables into a set of uncorrelated ones that better expose the various relationships among the original data items. At the same time, SVD is a method for identifying and ordering the dimensions along which data points exhibit the most variation. This ties in to the third way of viewing SVD, which is that, once we have identified where the most variation is, it's possible to find the best approximation of the original data points using fewer dimensions. Hence, SVD can be seen as a method for data reduction.

SVD is based on a theorem from linear algebra which says that a rectangular matrix $\boldsymbol{A}$ can be broken down into the product of three matrices - an orthogonal matrix $\boldsymbol{U}$, a diagonal matrix $\boldsymbol{\Sigma}$, and the transpose of an orthogonal matrix $\boldsymbol{V}$. The theorem is expressed by:

$$\boldsymbol{A}_{mn} = \boldsymbol{U}_{mm}\boldsymbol{\Sigma}_{mn}\boldsymbol{V}_{nn}^{T}\ , \tag{3.49}$$

where $\boldsymbol{U^T U = I, V^T V = I;}$ the columns of $\boldsymbol{U}$ are orthonormal eigenvectors of $\boldsymbol{A^T A}$, the columns of $\boldsymbol{V}$ are orthonormal eigenvectors of $\boldsymbol{A^T A}$, and $\boldsymbol{\Sigma}$ is a diagonal matrix containing the eigenvalues from $\boldsymbol{U}$ or $\boldsymbol{V}$ in descending order.

In particular, the SVD of the channel $\boldsymbol{H}$ can be written as $\boldsymbol{H = U\ \Sigma\ V}$, where $\boldsymbol{U}$ and $\boldsymbol{V}$ are unitary matrices and $\boldsymbol{\Sigma}$ is a diagonal matrix of positive eigenvalues. If the transmitter knows $\boldsymbol{V}$, it can precode the transmitted vector as $\boldsymbol{x} = \boldsymbol{V}^{*}\boldsymbol{s}$, where $\mathbf{s}$ is the information to be transmitted. The receiver then applies $\boldsymbol{U}^{*}$**,** resulting in a one-to-one tap mapping between transmit and receiver symbols with no cross terms:

$$\text{Transmitter processing} \begin{cases} \boldsymbol{r = H.x + n} \quad <=> \quad \boldsymbol{r = U.\Sigma.V.x + n} \\ <=> \ \boldsymbol{r = U.\Sigma.V.V^{*}s + n = U.\Sigma.s + n} \end{cases} \tag{3.50}$$

$$\text{Receiver processing ->} \quad <=> \ \tilde{\boldsymbol{s}} = \boldsymbol{\Sigma.s} + \tilde{\boldsymbol{n}}$$

If the channel matrix is completely known, singular value decomposition (SVD) precoding is known to achieve the MIMO channel capacity [5]. In this approach, the channel matrix is diagonalized by taking an SVD and removing the two unitary matrices through pre- and post-multiplication at the transmitter and receiver, respectively. Then, one data stream per singular value can be transmitted (with appropriate power loading) without creating any interference.

4

Iterative massive MIMO receivers

In this chapter the proposed receivers are introduced and explained. A set of performance results, based on Monte Carlo simulations, are presented and analyzed for the suggested scenarios.

The first experiment was, with a fixed number of R and T, to find the effect of the number of iterations in the receiver's performance. After that, we tested different numbers of transmitting and receiving antennas T and R in order to discover their effect in the number of errors. The ratio R/T was also taken in account to the experiments and different values were considered.

Each channel between transmit and receive antennas has 16 random gain, symbol-spaced multipath components with uncorrelated Rayleigh fading for different multipath components and different links (similar conclusions were observed for other channel models, provided that we have rich multipath propagation and small correlation between different channels). The BER results are expressed as a function of E_b/N_0, with E_b denoting the average bit energy for the set of R receive antennas (i.e., R times the bit energy for a single antenna) and N_0 denotes the unilateral power spectral density of the AWGN (Additive White Gaussian Noise) channel noise. For the sake of comparisons, we also include the ZF performance.

4.1 EGD/MRD + IB-DFE

To overcome the interference problem, is proposed the iterative receiver depicted in Fig. 4.1, where

$$\tilde{\boldsymbol{X}}_k = \boldsymbol{\psi} \boldsymbol{H}_{\boldsymbol{k}}^{\boldsymbol{H}} \boldsymbol{Y}_k + \boldsymbol{N}_k \,, \tag{4.1}$$

with $\boldsymbol{\psi}$ denoting a diagonal matrix whose *(t; t)*th element is given by

$$\boldsymbol{\psi}_{(t,t)} = \left(\sum_{k=0}^{N-1} \sum_{r=1}^{R} \left|\boldsymbol{H}_{\boldsymbol{k}}^{(\boldsymbol{r},\boldsymbol{t})}\right|^2\right)^{-1}, \tag{4.2}$$

i.e., it is an appropriate normalization parameter to ensure that the overall frequency response of the "channel plus receiver" for each MT has average 1 (a similar scaling is usually employed with IBDFE-based receivers [24]). The matrices $\boldsymbol{B}_k$ are employed to remove the residual ISI and inter-user interference. It can easily be shown that their optimum values are

$$\boldsymbol{B}_k = \boldsymbol{\psi} \boldsymbol{H}_{\boldsymbol{k}}^{\boldsymbol{H}} \boldsymbol{H}_k + \mathbf{I} \,. \tag{4.3}$$

This interference cancellation is done using

$$\overline{\mathbf{X}}_k = [\overline{\mathbf{X}}_0, \ldots, \overline{\mathbf{X}}_{N-1}] \,, \tag{4.4}$$

with $\overline{\mathbf{X}}_k$ denoting the frequency-domain average values conditioned to the FDE output for the previous iteration, which can be computed as described in [25].

Since for the first iteration we do not have information about the transmitted symbols and $\overline{\mathbf{X}}_k = 0$, our receiver can be regarded as a linear frequency-domain MRC. For the subsequent iterations we employ the average values conditioned to the receiver output at the previous iteration to remove the residual ISI and inter user interference. In general, for moderate-to-high SNR the average values conditioned to the receiver output approach the transmitted signals as we increase the number of iterations, which means that the interference cancellation performed by the $\mathbf{B}_k$ becomes more effective and the performance improves.

Moreover, since the average values conditioned to the receiver output can be regarded as soft decisions [25], this reduces significantly error propagation effects in our iterative receiver (in fact, we did not observe error propagation effects with our receiver). Other approximation that was also tested in this work was the EGC (Equal Gain Combiner) where and equal gain is given to every antenna combination. The only difference in practice to MRC is the matrix $\mathbf{B}_k$ whose values are calculated as

$$\boldsymbol{B}_k = \boldsymbol{\psi} \boldsymbol{A}_k^H \boldsymbol{H}_k + \mathbf{I}\,, \tag{4.5}$$

where $\boldsymbol{A}_k = \boldsymbol{H}_k^H$ for the MRC case and $\boldsymbol{A}_k = e^{j*\arg(\boldsymbol{H}_k^H)}$ for the EGC case.

This receiver showed to be more effective than MRC in schemes with a small number of communicating antennas.

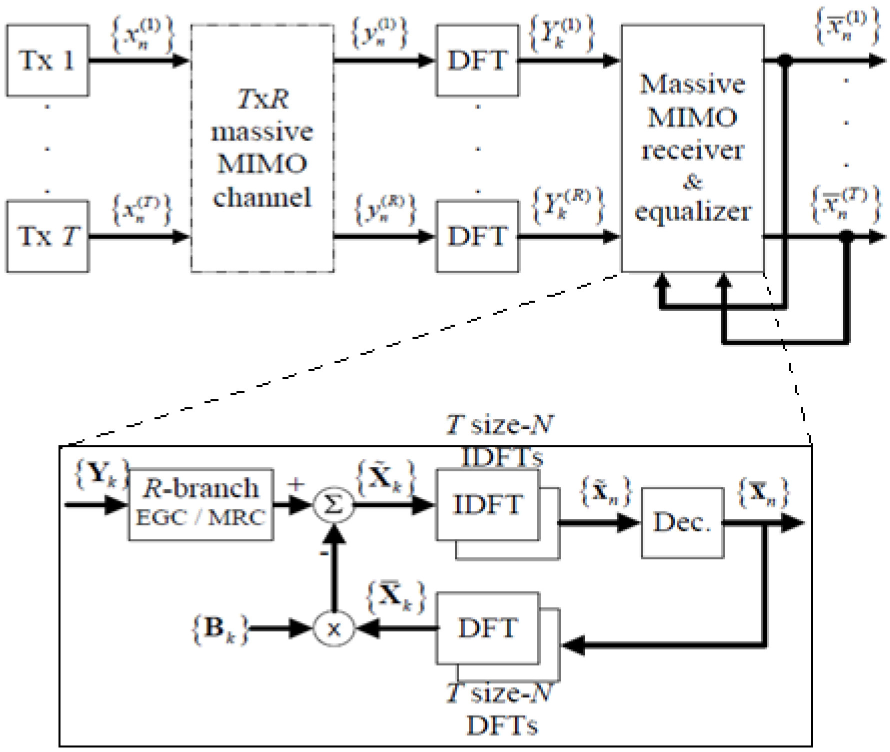

Fig. 4.1– Proposed receiver structure.

4.2 Performance results

Heterogeneous deployments are seen as a solution to cope with networks that have a high density of devices, which are characterized by high interference levels that may degrade the transmission – in this case the uplink.

The objective of this chapter is to evaluate the performance of the proposed receivers. The results of the simulations with different configurations are presented, so we can take conclusions about the effect of some parameters and different deployments. The terminology for receiving and transmitting antennas is 'RxT' where R are the receiving and T the transmitting ones.

4.2.1 Iterations effect

The following simulations were done to observe the effect of the iterations made by the iterative receivers to cancel interference, combined with different ratios between number of receiving and transmitting antennas. As scenarios we have some configurations: the number of transmitting antennas was kept constant as T=10, and the number of receiving antennas was changed between the values of 20, 50 and 100, producing a ratio R/T of 2, 5 and 10 respectively. Six interference cancelation iterations were done in each slot by each receiver.

Other configurations of number of antennas RxT were tested, nevertheless similar results were obtained and comparable to the presented results by their ratio R/T, i.e. the results obtained for one ratio were similar when the number of antennas changed in the same proportion, keeping the same ratio R/T.

By observation of the results we can conclude that the performance of the system increases when the receivers perform a higher number of iterations, but not in an unlimited way. In fact, just after a few iterations (let's say four), the performance of this system seems to converge to a certain 'limit'. This limit oscillates with the different scenarios of number of transmitting and receiving antennas and also dependent on the receiver employed. The performance of the proposed receivers in all simulated cases were equal or better than ZF the receiver after few iterations. Posterior simulations with a higher number of iterations (till 10) were tested and all the same conclusions were taken regarding those results.

4.2.1.1 Results of iterations effect on EGD

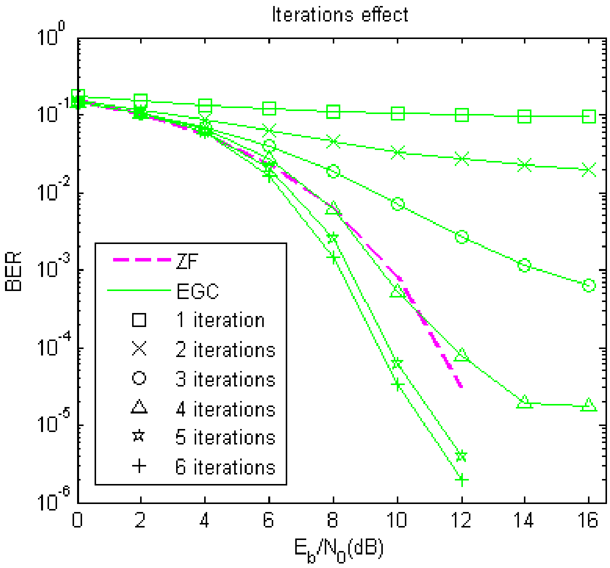

Fig 4.2 – Iterations effect on 20x10 EGD

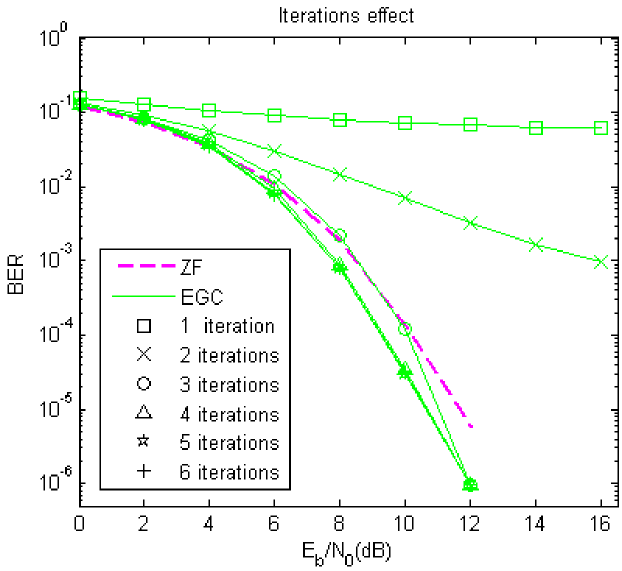

Fig 4.3– Iterations effect on 50x10 EGD

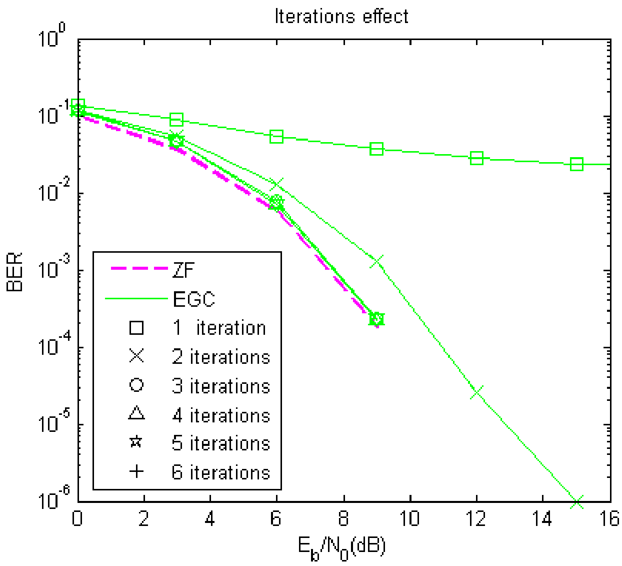

Fig 4.4 – Iterations effect on 100x10 EGD

In this set of simulations (Figs 4.2 - 4.4), where the applied receiver was IB-DFE combined with EGD, the effect of the number of iterations to cancel interference is very noticeable in the different scenarios. When the ratio *R/T* is low this effect improves the system performance until a high number of iterations (let's say all 6). Nevertheless, when the ratio *R/T* is bigger, the iterations starts to have less influence after the first ones (let's say 3) and the performance reaches a certain limit.

4.2.1.2 Results of iterations effect on MRD

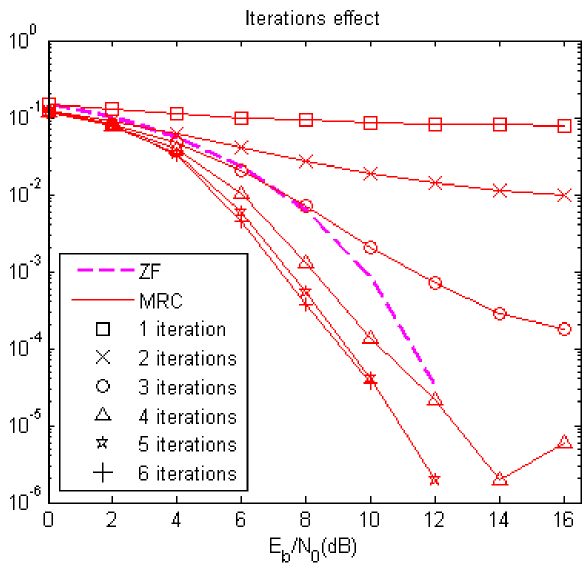

Fig 4.5– Iterations effect on 20x10 MRD

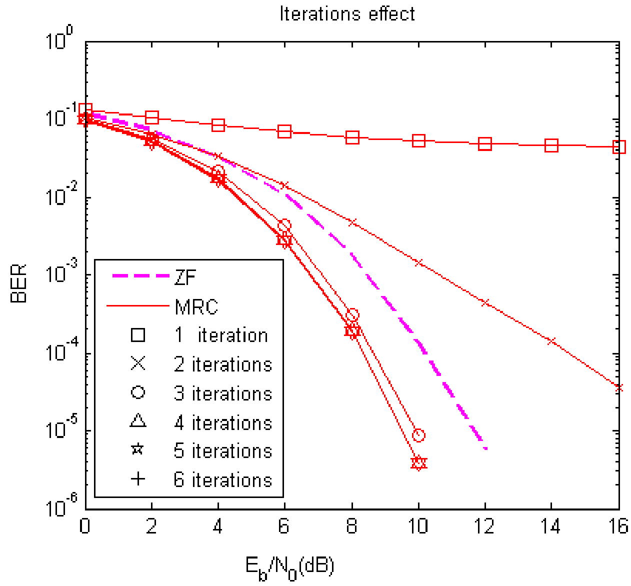

Fig 4.6– Iterations effect on 50x10 MRD

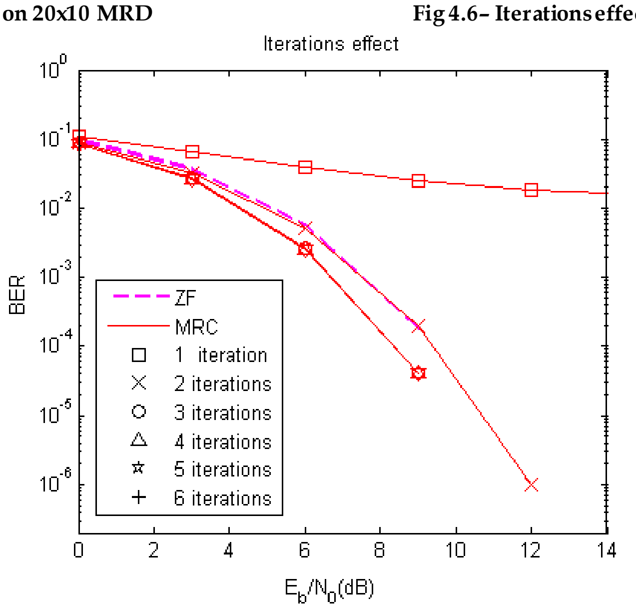

Fig 4.7– Iterations effect on 100x10 MRD

In this second set of results (Figs 4.5 - 4.7), this time the simulations were performed using an MRC based detector combined with IB-DFE. The results observed match the previous conclusions taken based on EGD+IB-DFE, where a bigger number of iterations are needed to achieve a certain performance limit using a low *R/T* antenna ratio, and less iterations are needed to achieve this limit for a bigger *R/T* ratio. The main difference for the previous receiver is the improved performance limit, which is observable by a lower BER. This improvement is due to the usage of an MRC algorithm instead of the EGC one.

4.2.1.3 Results of iterations effect on IB-DFE

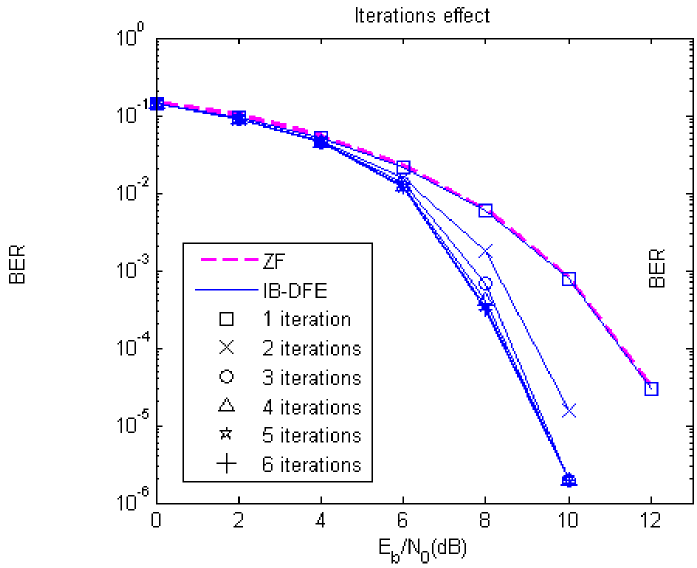

Fig 4.8– Iterations effect on 20x10 IB-DFE

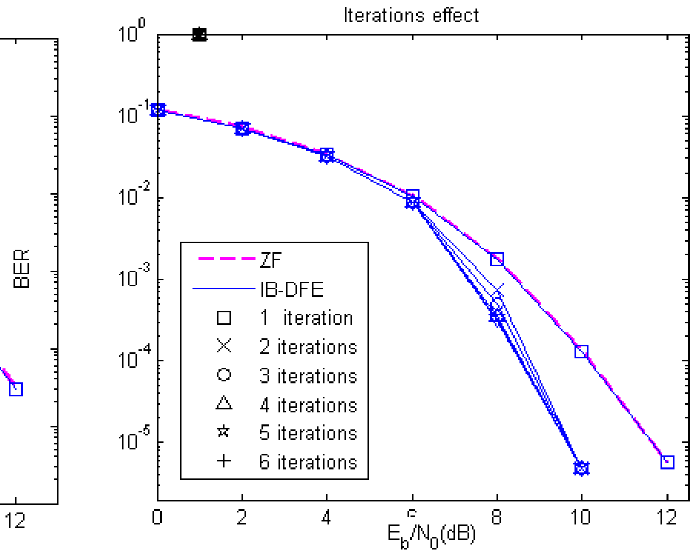

Fig 4.9– Iterations effect on 50x10 IB-DFE

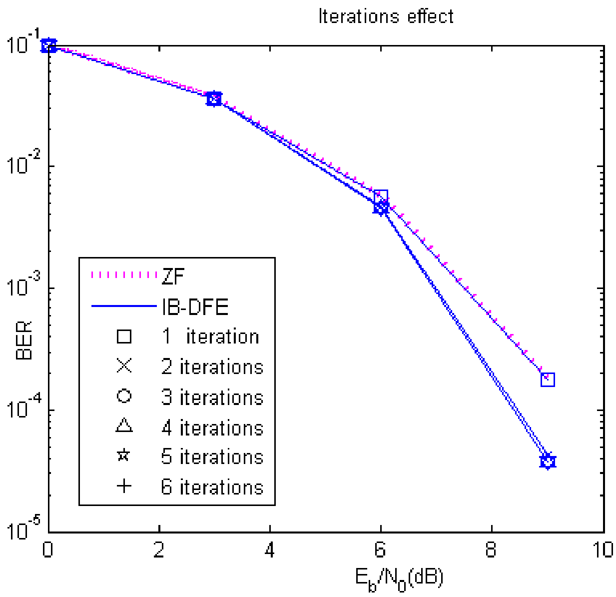

Fig 4.10 – Iterations effect on 100x10 IB-DFE

In this last set of simulations (Figs 4.8 - 4.10) which were performed using a conventional IB-DFE receiver, the results showed up not to follow the exact same conclusions taken before. With this receiver, the performance of the system was also improved, but just until the second iteration (in average) where a certain performance limit is reached. This inference is noticeable in all *RxT* configurations, and even more evident when the ratio *R/T* is bigger. The performance of this receiver in simulated cases was always equal or better than ZF the receiver.

4.2.2 Increasing number of antennas

4.2.2.1 Increasing ratio

In these simulations, whose results are presented in the Figs 4.11 to 4.13, the effect of different combinations of transmitting and receiving number of antennas was tested.

To start, the number of transmitting antennas was kept constant, T=10, and the number of receiving ones increased within the values of 10, 20, 50 and 100, producing ratios *R/T* of 1, 2, 5 and 10 respectively. With this simulation we can take conclusions about the effect of the increasing number of receiving antennas by itself, as well as the impact of different ratios R/T in the system's performance.

The number of interference cancelation iterations was chosen to be four, as it was observed to have a good performance. This value of iterations approached the best results achieved by the effect of increasing number of iterations, without compromising the complexity and delay with too many iterations.

Results of increasing ratio effect

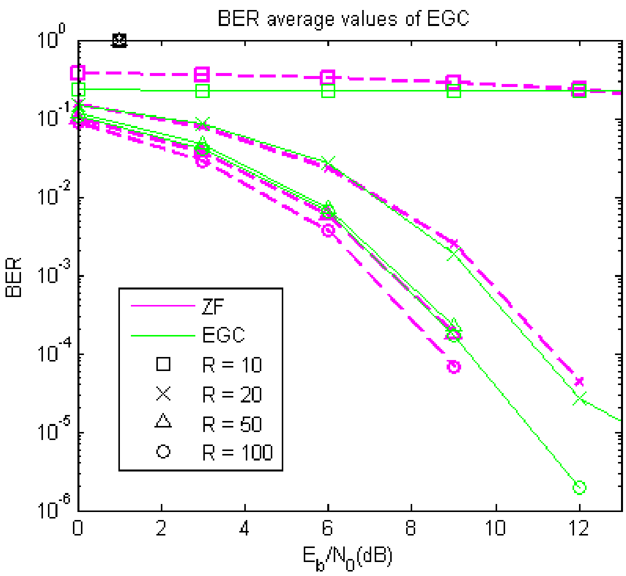

Fig 4.11 – Increasing ratio effect on EGC

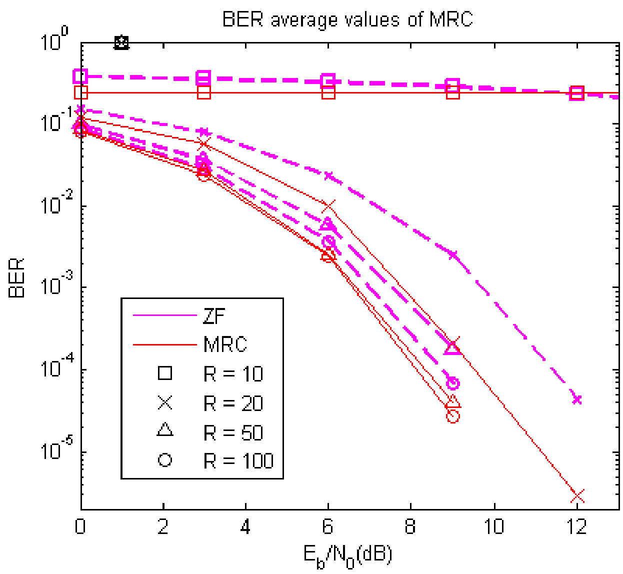

Fig 4.12 – Increasing ratio effect on MRC

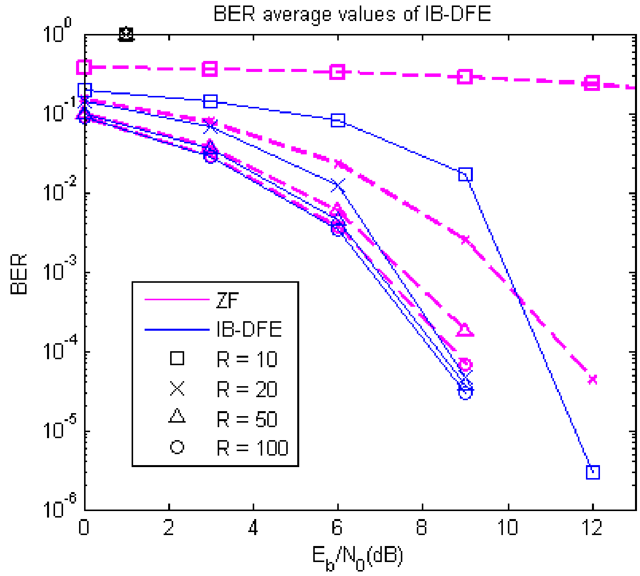

Fig 4.13 – Increasing ratio effect on IB-DFE

From these results, we can conclude that the performance of these receivers is improved when the ratio between receiving and transmitting antennas, *R/T*, has a higher value. Nevertheless, as observed in the iterations effect, this improvement doesn't grow without boundaries. In fact, we can see that the performance of a ratio *R/T* = 5, it's similar to the performance of a ratio *R/T* = 10. The next step was also increase the number of antennas but this time also in the transmitter side. This number *T* is always kept under *R*, as we don't want to have more data streams than receiving antennas.

4.2.2.2 Constant ratio

For these simulations the ratio between receiving and transmitting antennas was kept with a value of two, being the number of receiving antenna always twice as transmitting ones. Setting this ratio, different pairs of *RxT* antennas were tested. It was observed that when we increase the effective number of antennas with a constant *R/T* antennas ratio the performance of the system is also approximately constant. This takes us to the conclusion that the performance of the system, regarding number of antennas, doesn't depend on the overall number of them but just in the ratio between receiving and transmitting ones, *R/T*. The performance of the system is improved, to certain limits, with a higher value of this ratio, as observed in Figs 4.14, 4.15 and 4.16.

Other configurations of number of antennas *RxT* were tested for different constant ratios, nevertheless the same conclusion was taken, i.e. if the ration is constant, the performance will also be.

Results of increasing antennas effect – constant ratio

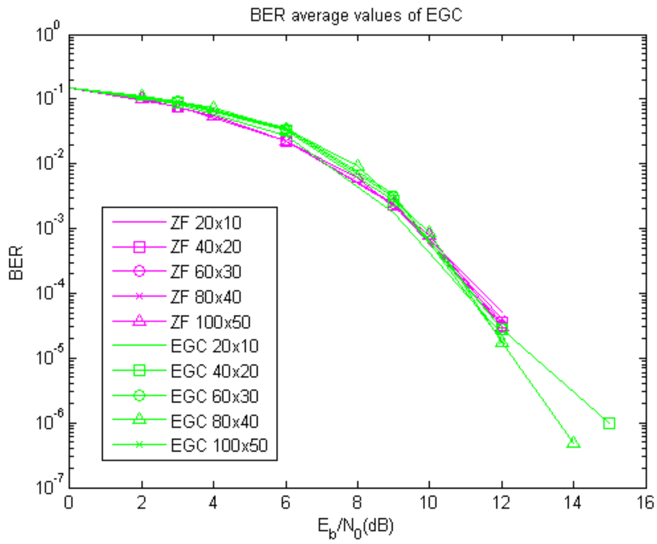

Fig 4.14 – Constant ratio effect on EGC

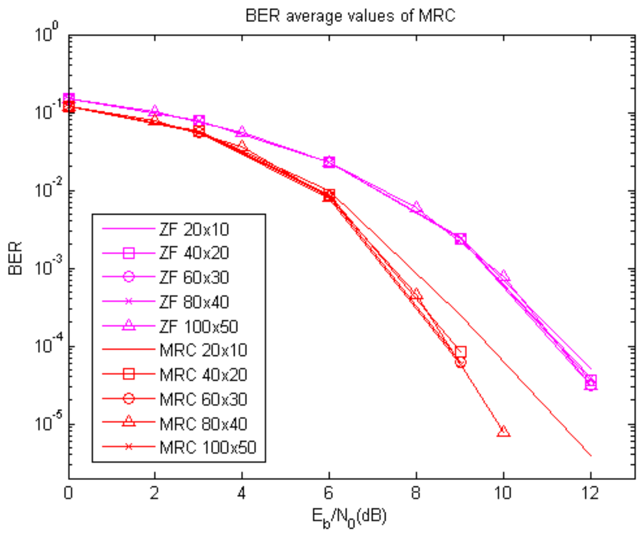

Fig 4.15 – Constant ratio effect on MRC

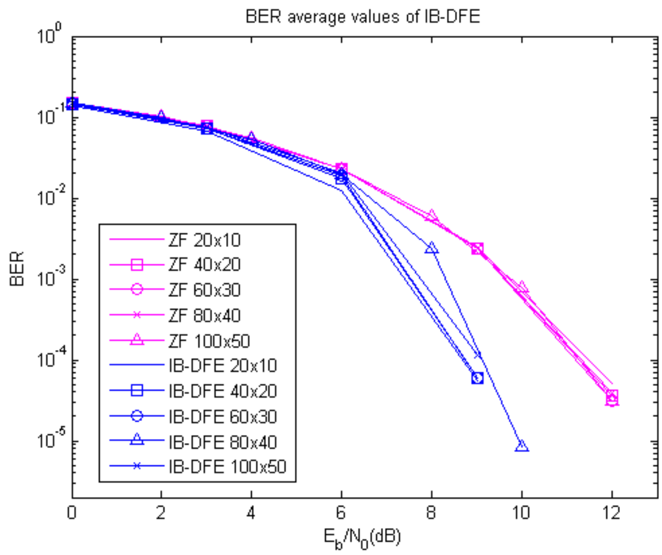

Fig 4.16 – Constant ratio effect on IB-DFE

4.2.2.3 Increasing transmitting antennas

For the last experiments, whose results are shown in the Figs 4.17, 4.18 and 4.19, the number of receiving antennas was defined with a high value, R=100, and the number of transmitting ones was increased from 10 to 30, 50, 60, 70 and 80. This simulations created some more different scenarios where we expected to take more conclusions about antennas configuration effect in system's performance. Also here, four interference cancelation iterations was the value chosen, for the same reasons mentioned before.

Results of increasing transmitting antennas

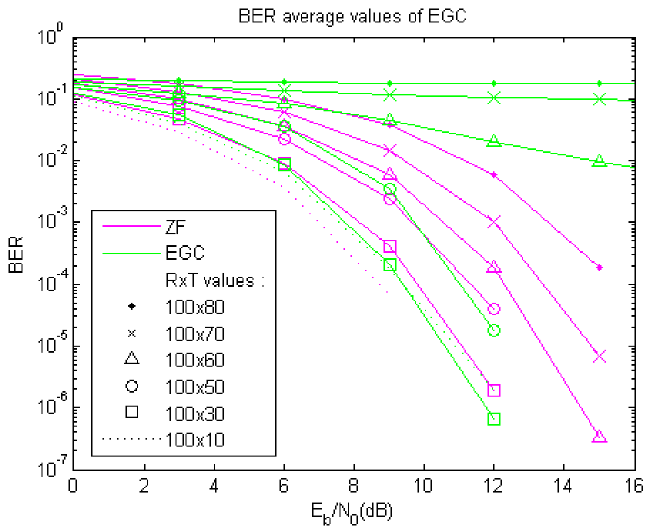

Fig 4.17 – Increasing transmitting antennas on EGC

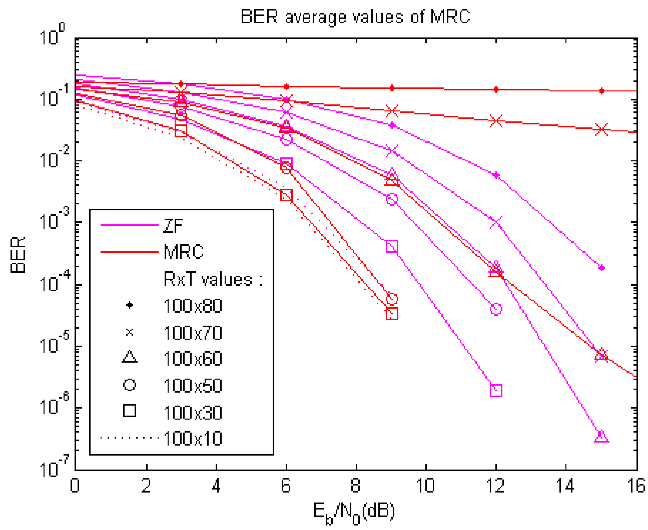

Fig 4.18 – Increasing transmitting antennas on MRC

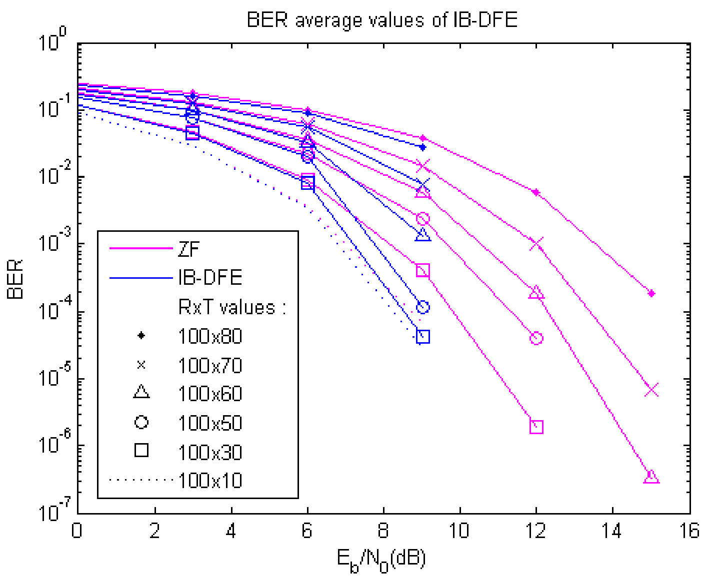

Fig 4.19 – Increasing transmitting antennas on IB-DFE

By maintaining the number of receiving antennas and making the number of transmitting ones changeable, also in these scenarios we produce different antennas ratio R/T. These simulated configurations are more likely to be found in practical terms, as in this thesis we deal with up-link. In other words, it's more probable in uplink to have a fixed number of receiving antennas and a fluctuating number of transmitting ones, as we can have mobile users connecting and disconnecting from the base station over time.

From all simulated scenarios, we can realize that the performance of this system is highly influenced by the ratio R/T, so in order to keep a good performance, this value of ratio should be maintained above a certain threshold. By other words, as we deal with the up-link and it's expected to have a fixed number of receiving antennas, we should limit the number of transmitting antennas (users) per base station, or to limit the overall transmitting antennas, in order to have a minimum required system's performance.

For the proposed iterative receivers, the ratio $R/T = 2$ seems to be a threshold value. From this value to the smallest ones, the system's performance starts to degrade in a very evident way. This effect is not noticeable when the receiver employed is the ZF one, as the performance in this case appears to be directly dependent on the ratio R/T. For the conventional IB-DFE receiver, the system's performance seems to get worse also in a related way as the ratio R/T decreases.

5

Conclusions

5.1 Final Considerations

In this chapter are presented the final considerations about the produced document, as well as some ideas of paths for future work and development.

Regarding the development of the 5G communications systems, massive MIMO are expected to have a major role in these ones. In order for these systems to work efficiently and to meet the 5G system's requirements, much work of development and improvement of techniques has to be done.

In this thesis, we just focused on a little piece of the puzzle which respects to the receiving techniques, equalization and interference cancelation for the uplink in a massive MIMO scenario. To develop and test these receiving techniques, much background work and development have been done, since the SC-FDE scheme, to the model of a massive MIMO communication system and the models of channel used.

The usage of this receivers in massive MIMO can mitigate the high computational load that these systems would require: to perform the receiving and equalization processes, if the different channel matrix inversions techniques were employed, huge channel matrix would have to be inverted and manipulated. Furthermore, the performance of these introduced techniques can still achieve a good performance with just few iterations, in comparison to more commonly used techniques.

The overall number or antennas was not the main effect analyzed in this experiments. Based on the realized simulations, it's the ratio R/T that shows to have the major influence in the massive MIMO communication system's performance. In particular, regarding the proposed receivers, the value of this ratio should be above $R/T = 2$, as if the values is lower than this, the system's performance degrades abruptly. There seems to be also an upper bound near $R/T = 5$, where the system's performance appears to reach a lower bound for BER.

5.2 Future Work

About the next steps to take on this path of work, the suggestion is to make a deeper mathematical analysis of these systems to understand where there is still margin to improve performance and/or to decrease complexity.

Even more detailed channel models and information about channel capacity can help to improve and decide which approach fit's better these massive MIMO scenarios, and which get closer to the system's optimal performance.

In these thesis we just evaluated some specific receivers' performance, therefore a broader analysis and simulations about receiving and equalization techniques can be done for these massive MIMO schemes.

A receiver based in SVD algorithm was also developed, but it was not enough tested and analyzed within the duration of this thesis. The extension of these simulations and analysis could produce more results and conclusions.

As we can conclude, the different network scenarios seem to be a major issue for the future of these systems combined with the presented receivers, as the ratio R/T deeply influences the system's performance. If similar results will be taken for different receivers and scenarios, good device and network planning will be needed.

Attachments

An MRC-Based Receiver for SC-FDE Modulations with Massive MIMO Schemes

David Borges, Rui Dinis, Paulo Montezuma

Abstract - Nowadays we are watching a big and fast grow of the Internet usage, so the needs of data transference are growing. As a consequence of the increasing number of users, the spectrum is getting overloaded with communications, increasing the interference. Therefore a different path of ideas has been followed and the communication process has been taken to the next level by the usage of big arrays of antennas and multi-stream communication (MIMO systems).

These systems can be combined with an SC-FDE (Single-Carrier Frequency Domain Equalization) scheme to improve the power efficiency due to the low envelope fluctuations. In this paper we will focus on the equalization field, more specifically in the FDE (Frequency Domain Equalization), studying the performance of different approaches, namely ZF (Zero Forcing), EGC (Equal Gain Combiner), MRC (Maximum Ratio Combiner), IB-DFE (Iterative Block Decision Feedback Equalizer) and a proposed receiver combining MRC (or EGC) and IB-DFE.

I. Introduction

Massive MIMO schemes (Multiple-Input, Multiple-Output) involving several tens or even hundreds of antenna elements are expected to be central technologies for 5G systems [1].

As a direct consequence of the increase in data rates, the effects of multi-path propagation and inter symbol interference (ISI) have been augmented, resulting in the need for more complex equalizers. The complexity of the equalization process is enlarged even more in MIMO systems due to the addition of extra transmit and receive antennas [**?**].

Block transmission techniques have been used intensively due to their performance in high data rate transmission over severely time-dispersive channel. The two alternatives are OFDM (Orthogonal Frequency Division Multiplexing) and Single Carrier (SC) modulation using FDE. In this paper we will use the SC-FDE technique which is more suitable for uplink due to its lower PAPR (Power to Average Power Ratio).

Although these techniques allow huge capacity gains, the implementation complexity precludes the use of conventional MIMO detection schemes [2]. For this reason, massive MIMO schemes should avoid the usual matrix inversion inherent to MIMO receivers, which makes receivers based on the MRC (Maximum Ratio Combining) particularly interesting.

In the equalization field, an innovative and promising IFDE (Iterative FDE) technique for SC-FDE, denoted IB-DFE was developed in previous work and used in this work. These IFDE receivers can be regarded as iterative DFE receivers with the feed-forward and the feedback operations implemented in the frequency domain. Since the feedback loop takes into account not just the hard decisions for each block but also the overall block reliability, error propagation is reduced.

Consequently, IFDE techniques offer much better performance than non-iterative methods. The equalization and channel decoding procedures are mostly done in separately (i.e., the feedback loop uses the equalizer outputs instead of the channel decoder outputs), although it is know that higher performance gains can be achieved if these procedures are done at the same time. One example of this implementation are the turbo equalization schemes, where these two actions are repeated in an iterative way. Turbo-equalizers were first proposed for time-domain receivers but they also allow frequency domain usage [**?**].

A low-complexity iterative frequency-domain receiver based on the MRC (Maximum Ratio Combining) approach is proposed. This receiver does not require matrix inversions and has excellent performance, being able to approach the MFB (Matched Filter Bound) after just a few iterations, even for a moderate number of antennas.

In this paper we will consider a MIMO SC FDE communication scheme and study the impact of the number of used antennas in sender and receiver in the BER (Bit Error Rate) values, as well as the performance of different FDE?s approaches in BER values.

II. System Characterization

We consider the multi-user massive MIMO scenario pictured in fig. 1 which characterizes the up-link transmission between T single-antenna MT and a BS (Base Station) with $R >> T$ receive antennas (the generalization for the case where we have multiple antennas at the MTs is straightforward). The channels between each transmit and receive antenna are assumed to be severely time-dispersive and an SC-FDE transmission technique is employed by each MT.

The tth MT transmits the block of N data symbols $\{x_n^{(t)}; n = 0, 1, ..., N-1\}$ and the received block at the rth BS antenna is $\{y_n^{(r)}; k = 0, 1, ..., N-1\}$ (as with other SC-FDE schemes, an appropriate cyclic prefix is appended to each transmitted block and removed at the receiver). When appropriate cyclic prefixes are employed the corresponding frequency-domain block $\{Y_k^{(r)}; k = 0, 1, ..., N-1\}$ satisfies

$$\mathbf{Y}_k = \left[Y_k^{(1)} \; ... \; Y_k^{(R)}\right]^T = \mathbf{H}_k\mathbf{X}_k + \mathbf{N}_k, \qquad (1)$$

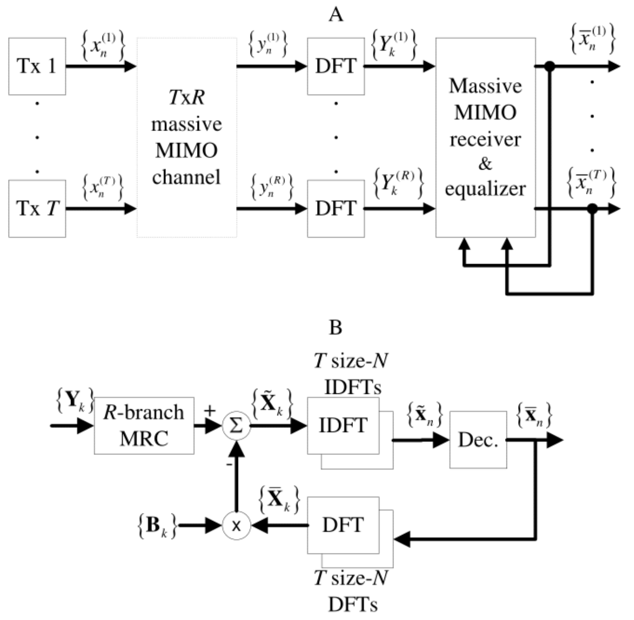

Fig. 1. Overall massive MIMO system for SC-FDE schemes (A) and detail of the massive MIMO receiver and equalization (B).

where $\mathbf{H}_k$ denotes the $R \times T$ channel matrix for the kth frequency, with (r,t)th element $H_k^{(r,t)}$, $\mathbf{X}_k = \left[X_k^{(1)} \ ... \ X_k^{(T)}\right]^T$ and $\mathbf{N}_k$ denotes the channel noise. For a linear MMSE-based (Minimum Mean Squared Error) receiver the data symbols can be obtained from the IDFT of the block $\{\tilde{X}_k^{(t)}; k = 0, 1, ..., N-1\}$, where

$$\tilde{\mathbf{X}}_k = [\tilde{X}_k^1 ... \tilde{X}_k^{(R)}]^T = \left(\mathbf{H}_k \mathbf{H}_k^H + \alpha \mathbf{I}\right)^{-1} \mathbf{H}_k^H \mathbf{X}_k, \quad (2)$$

(see details in [6], e.g.), where $\mathbf{I}$ is an appropriate identity matrix and $\alpha = E[|N_k^{(r)}|^2]/E[|X_k^{(t)}|^2]$ is assumed identical for all values of t and r. However, this involves the inversion of a matrix for each frequency, and the dimensions of these matrices can be very high in massive MIMO systems. Massive MIMO schemes usually employ simpler receivers. The most popular are probably the ones based on the MRC [2]. These receivers take advantage of the fact that

$$\mathbf{H}_k^H \mathbf{H}_k \approx R\mathbf{I}, \quad (3)$$

an approximation that is accurate when $R >> 1$ (i.e., for massive MIMO systems), provided that the channels between different transmit and receive antennas have small correlation.

For SC-FDE we could employ a frequency-domain receiver with MRC at each frequency, based on $\mathbf{H}_k^H \mathbf{Y}_k$. However, the residual interference levels can still be substantial, especially for moderate values of R/T.

To overcome this problem, propose the iterative receiver depicted in fig. 1(B), where

$$\tilde{\mathbf{X}}_k = \mathbf{\Psi} \mathbf{H}_k^H \mathbf{Y}_k - \mathbf{B}_k \overline{\mathbf{X}}_k, \quad (4)$$

with $\mathbf{\Psi}$ denoting a diagonal matrix whose (t,t)th element is given by $\left(\sum_{k=0}^{N-1} \sum_{r=1}^{R} |H_k^{(r,t)}|^2\right)^{-1}$, i.e., it is an appropriate normalization parameter to ensure that the overall frequency-response of the "channel plus receiver" for each MT has average 1 (a similar scaling is usually employed with IB-DFE-based receivers [3], [4]). The matrices $\mathbf{B}_k$ are employed to remove the residual ISI and inter-user interference. It can easily be shown that their optimum values are

$$\mathbf{B}_k = \mathbf{\Psi} \mathbf{H}_k^H \mathbf{H}_k - \mathbf{I}. \quad (5)$$

This interference cancellation is done using $\overline{\mathbf{X}}_k = \left[\overline{X}_0 ... \overline{X}_{N-1}\right]$, with $\overline{X}_k$ denoting the frequency-domain average values conditioned to the FDE output for the previous iteration, which can be computed as described in [6] .

Since for the first iteration we do not have information about the transmitted symbols and $\overline{\mathbf{X}}_k = \mathbf{0}$, and our receiver can be regarded as a linear frequency-domain MRC. For the subsequent iterations we employ the average values conditioned to the receiver output at the previous iteration to remove the residual ISI and inter user interference. In general, for moderate-to-high SNR (Signal-to-Noise Ratio) the average values conditioned to the receiver output approach the transmitted signals as we increase the number of iterations, which means that the interference cancellation performed by the $\mathbf{B}_k$ becomes more effective and the performance improves. Moreover, since the average values conditioned to the receiver output can be regarded as soft decisions [6], this reduces significantly error propagation effects in our iterative receiver (in fact, we did not observe error propagation effects with our receiver).

Other approximation that was also tested in this work was the EGC (Equal Gain Combiner) where and equal gain is given to every antenna combination. The only difference in practice to MRC is the matrix $\mathbf{B}_k$ whose values are calculated as

$$\mathbf{B}_k = \mathbf{\Psi} \mathbf{A}_k^H \mathbf{H}_k - \mathbf{I}. \quad (6)$$

This receiver showed to be more effective than MRC in schemes with a small number of communicating antennas.

III. Performance Results

In this section we present a set of performance results for the proposed receiver. We considered data blocks with $N = 256$ QPSK (Quaternary Phase Shift Keying) data symbols per block. The first experiment was, with a fixed number of R and T, to find the effect of the number of iterations in the receiver's performance. After that, we tested different numbers of transmitting and receiving antennas T and R in order to discover their effect in the number of errors. The ration R/T was also taken in account to the experiments and different values were considered. Each channel between transmit and receive antennas has 16 equal-power, symbol-spaced multipath components with uncorrelated Rayleigh fading for different multipath components and different links (similar conclusions were observed for other channel models, provided that we have rich multipath propagation and and small correlation between different channels).

The BER results are expressed as a function of E_b/N_0, with E_b denoting the average bit energy for the set of R receive antennas (i.e., R times the bit energy for a single antenna) and N_0 denotes the unilateral power spectral density of the AWGN (Additive White Gaussian Noise) channel noise. For the sake of comparisons, we also include the MFB and ZF performance.

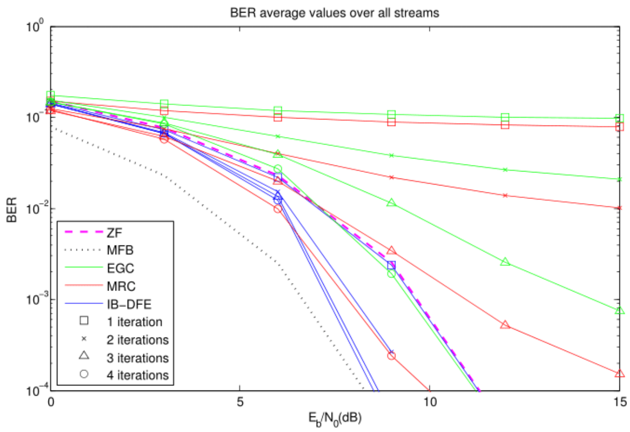

Fig. 2. BER performance for the proposed iterative FDE techniques when $R = 20$ and $T = 10$.

Fig. 2 shows the BER (Bit Error Rate) performance for a BS with $R = 20$ receiving antennas and $T = 10$ transmitting antennas. The objective in this experience was to observe the effect of different number of iterations in the receiver. We can observe the performance of the different receivers increasing and being able to approach the MFB after just 4 iterations.

In Fig. 3, Fig. 4 and Fig. 5 we can notice the effect of the increasing number of transmitting and receiving antennas in the three different equalization techniques. Since we have more channels of communication transmitting data, this information will be taken in account when the equalization is made. This will result in a bigger combination of data which will decrease the number of errors in the receiver. This effect is visible in the three different type of receivers, but depending on the number of antennas, some techniques will more adapted. In this experiment, fixing the number of iterations to 4, we concluded that when the number of antennas is relatively low (less than 10) these approach has better results than MRC (IB-DFE has better performance but it requires matrices inversions). For a higher number of antennas, MRC turned up to be the best technique to use, approaching very closely the MFB.

IV. Conclusions

A promising low-complexity detection technique for SC-FDE modulations with massive MIMO schemes was proposed in this letter. This technique, which is based on the MRC, does not require matrix inversions and has excellent performance. In fact, our receiver is able to approach the MFB after just a few iterations, even for a moderate number of antennas.

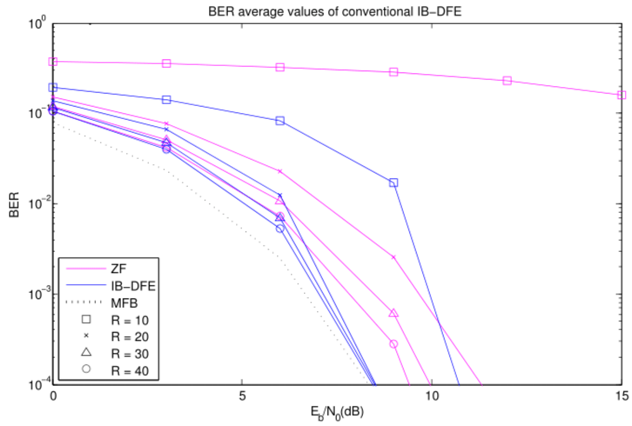

Fig. 3. BER performance for the proposed IB-DFE receiver when $T = 10$ and 4 iterations done.

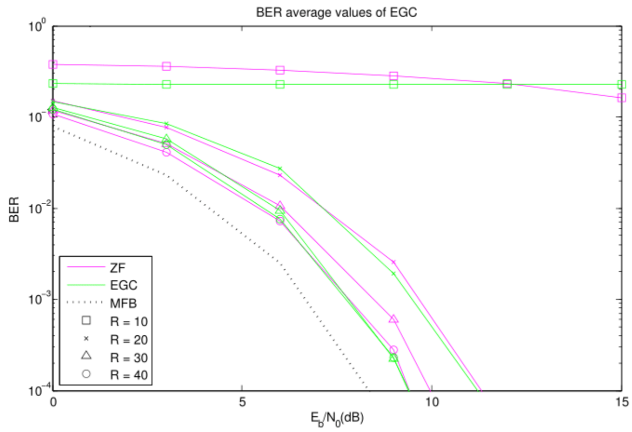

Fig. 4. BER performance for the proposed EGC receiver when $T = 10$ and 4 iterations done.

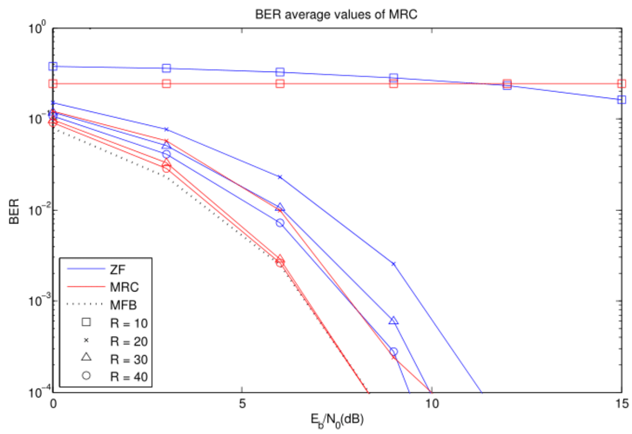

Fig. 5. BER performance for the proposed MRC receiver when $T = 10$ and 4 iterations done.

References

[1] F. Boccardi, R. Heath, A. Lozano, T. Marzetta, P. Popovski, "Five disruptive technology directions for 5G", IEEE Communications Magazine,

Vol. 52, No. 2, pp.74-80, Feb. 2014.
[2] F. Rusek, D. Persson, B. K. Lau, E. G. Larsson, O. Edfors, F. Tufvesson, and T. L. Marzetta, ”Scaling up MIMO: opportunities and challenges with very large arrays”, IEEE Signal Processessing Magazine, Vol. 30, No. 1, pp. 40-60, Jan. 2013.
[3] N. Benvenuto and S. Tomasin, ”Block iterative dfe for single carrier modulation”, Electron. Lett., vol. 39, no. 19, pp. 11441145, Sep. 2002.
[4] R.Dinis, R.Kalbasi, D.Falconer and A.Banihashemi, ”Iterative Layered Space- Time Receivers for Single-Carrier Transmission over Severe Time-Dispersive Channels”, IEEE Comm. Letters, Vol. 8, No. 9, pp. 579-581, Sep.2004.
[5] N. Benvenuto, R. Dinis, D. Falconer, S. Tomasin, ”Single Carrier Modulation With Nonlinear Frequency Domain Equalization: An Idea Whose Time Has Come - Again”, Proceedings of the IEEE, vol. 98, no.1, pp.69-96, Jan. 2010.
[6] P. Silva, R. Dinis, *Frequency-Domain Multiuser Detection for CDMA Systems*, River Publishers, Aalborg, 2012.

BIBLIOGRAPHY

[1] I. T. W. C. Systems, “Introduction to wireless communication systems,” 2010.

[2] G. Channel, “Harvard SEAS ES250 – Information Theory.”

[3] A. Gusmao, R. Dinis, J. Conceicao, and N. Esteves, “Comparison of two modulation choices for broadband wireless communications,” in *VTC2000-Spring. 2000 IEEE 51st Vehicular Technology Conference Proceedings (Cat. No.00CH37026)*, 2000, vol. 2, pp. 1300–1305.

[4] “A WCDMA Air Interface Part 2: 1 of 21 WCDMA Air Interface Training Part 2 CDMA Power Control, RAKE Receiver, and Soft Handover. - Documents.” [Online]. Available: http://documentslide.com/documents/2038-13-enlzu-108-5306-rev-a-wcdma-air-interface-part-2-1-of-21-wcdma.html.

[5] *Precoding Techniques for Digital Communication Systems*. Boston, MA: Springer US, 2008.

[6] Z. Pi and F. Khan, “An introduction to millimeter-wave mobile broadband systems,” *IEEE Commun. Mag.*, vol. 49, no. 6, pp. 101–107, Jun. 2011.

[7] F. Boccardi, R. Heath, A. Lozano, T. Marzetta, and P. Popovski, “Five disruptive technology directions for 5G,” *IEEE Commun. Mag.*, vol. 52, no. 2, pp. 74–80, Feb. 2014.

[8] T. S. Rappaport, S. Shu Sun, R. Mayzus, H. Hang Zhao, Y. Azar, K. Wang, G. N. Wong, J. K. Schulz, M. Samimi, and F. Gutierrez, “Millimeter Wave Mobile Communications for 5G Cellular: It Will Work!,” *IEEE Access*, vol. 1, pp. 335–349, 2013.

[9] S. Han, C. I, Z. Xu, and C. Rowell, “Large-scale antenna systems with hybrid analog and digital beamforming for millimeter wave 5G,” *IEEE Commun. Mag.*, vol. 53, no. 1, pp. 186–194, Jan. 2015.

[10] L. Lili Wei, R. Hu, Y. Yi Qian, and G. Geng Wu, “Key elements to enable millimeter wave communications for 5G wireless systems,” *IEEE Wirel. Commun.*, vol. 21, no. 6, pp. 136–143, Dec. 2014.

[11] A. Alkhateeb, J. Mo, N. González-Prelcic, and R. W. Heath, “MIMO precoding and combining solutions for millimeter-wave systems,” *IEEE Commun. Mag.*, vol. 52, no. 12, pp. 122–131, Dec. 2014.

[12] D. Choudhury, I. Labs, and I. Corporation, “5G Wireless and Millimeter Wave Technology Evolution : An Overview,” pp. 0–3, 2015.

[13] "MIMO." [Online]. Available: https://en.wikipedia.org/wiki/MIMO.

[14] E. G. Larsson, O. Edfors, F. Tufvesson, and T. L. Marzetta, "Massive MIMO for Next Generation Wireless Systems," pp. 1–20, 2013.

[15] T. L. Marzetta, "Noncooperative Cellular Wireless with Unlimited Numbers of Base Station Antennas," *IEEE Trans. Wirel. Commun.*, vol. 9, no. 11, pp. 3590–3600, Nov. 2010.

[16] J. Vieira, S. Malkowsky, K. Nieman, Z. Miers, N. Kundargi, L. Liu, I. Wong, V. Owall, O. Edfors, and F. Tufvesson, "A flexible 100-antenna testbed for Massive MIMO," in *2014 IEEE Globecom Workshops (GC Wkshps)*, 2014, pp. 287–293.

[17] "Single-carrier FDMA - Wikipedia, the free encyclopedia." [Online]. Available: https://en.wikipedia.org/wiki/Single-carrier_FDMA.

[18] T. Walzman and M. Schwartz, "Automatic equalization using the discrete frequency domain," *IEEE Trans. Inf. Theory*, vol. 19, no. 1, pp. 59–68, Jan. 1973.

[19] C. Silva, R. Dinis, and N. Souto, "MIMO SC-FDE Transmission Techniques with Channel Estimation and High-order Modulations," pp. 105–112, 2013.

[20] "LTE Up-link & SC-FDMA | ExploreGate." [Online]. Available: https://www.exploregate.com/video.aspx?video_id=55.

[21] F. Rusek, D. Persson, B. K. Lau, E. G. Larsson, T. L. Marzetta, O. Edfors, and F. Tufvesson, "Scaling up MIMO : Opportunities and challenges with very large arrays," *IEEE Signal Process. Mag.*, vol. 30, no. 1, pp. 40–60, 2013.

[22] M. K. Simon and M.-S. Alouini, *Digital Communication over Fading Channels*. Wiley-Interscience, 2007.

[23] N. Benvenuto and S. Tomasin, "Block iterative DFE for single carrier modulation."

[24] R. Dinis, R. Kalbasi, D. Falconer, and A. H. Banihashemi, "Iterative Layered Space-Time Receivers for Single-Carrier Transmission Over Severe Time-Dispersive Channels," *IEEE Commun. Lett.*, vol. 8, no. 9, pp. 579–581, Sep. 2004.

[25] P. Silva and R. Dinis, "Frequency-Domain Multiuser Detection for Highly Overloaded DS-CDMA Systems," in *2011 IEEE Vehicular Technology Conference (VTC Fall)*, 2011, pp. 1–5.

LOMBADA

Low complexity detection for SC-FDE massive MIMO systems

David Borges

2016